



1

2 **Overcoming barriers to enable convergence research by integrating ecological**
3 **and climate sciences: The NCAR-NEON system Version 1**

4

5 Danica L. Lombardozi^{1§}, William R. Wieder^{1,2,§*}, Negin Sobhani¹, Gordon B. Bonan¹, David Durden³,

6 Dawn Lenz³, Michael SanClements³, Samantha Weintraub-Leff³, Edward Ayres³, Christopher R. Florian³,

7 Kyla Dahlin⁴, Sanjiv Kumar⁵, Abigail L. S. Swann⁶, Claire Zarakas⁶, Charles Vardeman⁷, Valerio

8 Pascucci⁸

9

10 ¹ Climate and Global Dynamics Laboratory, National Center for Atmospheric Research, Boulder CO, USA.

11 ² Institute of Arctic and Alpine Research, University of Colorado Boulder, Boulder CO, USA.

12 ³ National Ecological Observatory Network, Battelle. Boulder CO, USA.

13 ⁴ Michigan State University, East Lansing MI, USA.

14 ⁵ College of Forestry, Wildlife and Environment, Auburn University, Auburn AL, USA.

15 ⁶ University of Washington, Seattle WA, USA.

16 ⁷ Center for Research Computing, University of Notre Dame, Notre Dame, IN, USA

17 ⁸ Scientific Computing and Imaging Institute, University of Utah, Salt Lake City, UT, USA

18 [§] Contributed equally as lead authors.

19 * Correspondence to: dll@ucar.edu and wwieder@ucar.edu

20



21 **Abstract**

22 Global change research demands a convergence among academic disciplines to understand
23 complex changes in Earth system function. Limitations related to data usability and computing
24 infrastructure, however, present barriers to effective use of the research tools needed for this cross-
25 disciplinary collaboration. To address these barriers, we created a computational platform that pairs
26 meteorological data and site-level ecosystem characterizations from the National Ecological Observatory
27 Network (NEON) with the Community Terrestrial System Model (CTSM) that is developed with university
28 partners at the National Center for Atmospheric Research (NCAR). This NCAR-NEON system features a
29 simplified user interface that facilitates access to and use of NEON observations and NCAR models. We
30 present preliminary results that compare observed NEON fluxes with CTSM simulations and describe
31 how the collaboration between NCAR and NEON that can be used by the global change research
32 community improves both the data and model. Beyond datasets and computing, the NCAR-NEON
33 system includes tutorials and visualization tools that facilitate interaction with observational and model
34 datasets and further enable opportunities for teaching and research. By expanding access to data,
35 models, and computing, cyberinfrastructure tools like the NCAR-NEON system will accelerate integration
36 across ecology and climate science disciplines to advance understanding in Earth system science and
37 global change.

38 **Short Summary**

39 We present a novel cyberinfrastructure system that uses National Ecological Observatory Network
40 measurements to run Community Terrestrial System Model point simulations in a containerized system.
41 The simple interface and tutorials expand access to data and models used in Earth system research by
42 removing technical barriers and facilitating research, educational opportunities, and community
43 engagement. The NCAR-NEON system enables convergence of climate and ecological sciences.

44 **1. Introduction**

45 Earth system science aims to deepen understanding of interactions between natural and social
46 systems and their responses to global change. As such, the collective understanding of changes in Earth
47 system function in response to global change drivers requires a convergence among scientific disciplines,
48 including physical and natural sciences (Kyker-Snowman et al. 2022). This research combines a variety
49 of complex observational data with ever more sophisticated computational models. Notably, Earth System
50 Models (ESMs) are essential tools for assessing and predicting our changing environment (Bonan and
51 Doney 2018), but limitations related to data usability and access to computing infrastructure present
52 barriers to effective use of these research tools (Fer et al. 2021). Addressing these barriers is critical to
53 engage the broad, cross-disciplinary communities that are required for Earth system science research,



54 education, and training (NASEM, 2022). We feel that tractable progress can be made to reduce these
55 data and technical barriers to better understand and project changes in Earth system function under
56 global change.

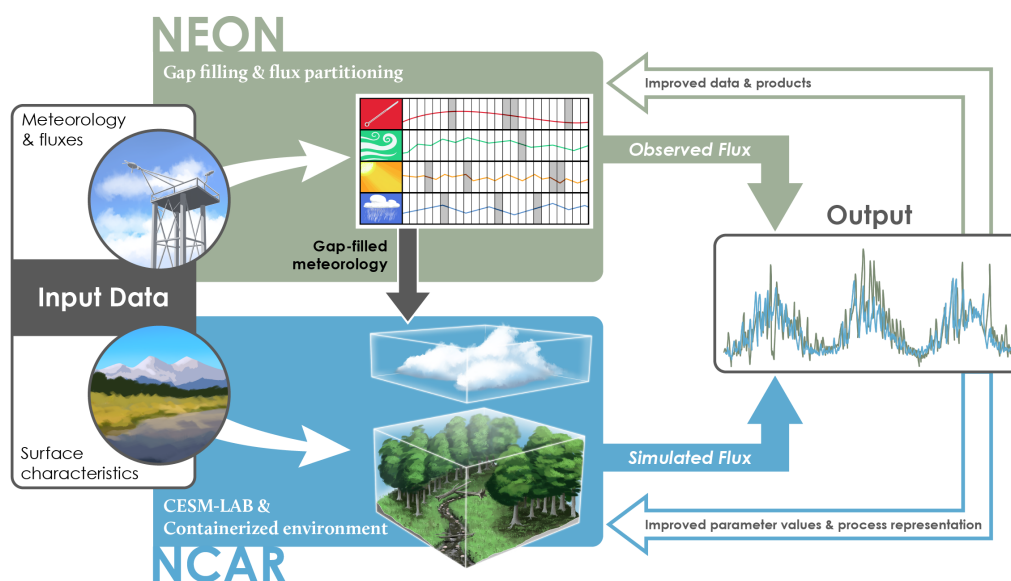
57 The availability, discoverability, and usability of observational data are essential to running,
58 calibrating, and validating models. For example, the scientific advancements made in measuring eddy
59 covariance (EC) fluxes have been critical to the development, evaluation, and improvement of the
60 representation of terrestrial ecosystems in ESMs. Initially, model-data comparisons were limited to short,
61 intensive field campaigns extending over a few weeks (Bonan et al. 1997), but this grew to comparison
62 with flux network datasets extending over several years at multiple sites (Stöckli et al. 2008), and
63 comparison with globally gridded flux products (Bonan et al. 2011; Jung et al. 2020). Flux tower data sets
64 continue to provide essential information for land model development and evaluation (Best et al. 2015;
65 Lawrence et al. 2019). Notably, single-point simulations can use EC measurements to facilitate more
66 rapid model development and testing of ecological hypotheses (Bonan et al. 2012; Burns et al 2018;
67 Swenson et al. 2019; Wieder et al. 2017). An explosion of EC measurements and strong network
68 coordination make these data easier to find (Durden et al. 2020; Pastorello et al. 2020), but the need to
69 perform additional data processing prior to use presents barriers to integrating ecological observations
70 into land model development and evaluation. These barriers include gap filling associated meteorological
71 data, assessing EC flux data quality, and persistent challenges in discovering and harmonizing
72 complementary data – including information about vegetation and soils at EC tower sites. Our work seeks
73 to provide a framework to address these data challenges to facilitate the integration of local meteorology,
74 EC flux measurements, and ecosystem characterizations in the development and evaluation of land
75 models that are used for Earth system prediction and global change research.

76 Beyond these data challenges, barriers to accessing and using computing infrastructure also
77 impede broader community engagement with tools that are central to global change research. This limits
78 the participation of scientists from environmental science and ecology, which are fundamental
79 components of the Earth system, in the development and use of ESMs. The Community Earth System
80 Model (CESM; Hurrell et al. 2013; Danabasoglu et al. 2020) has a long history of being freely and openly
81 available to users, yet several barriers related to training, cyberinfrastructure, and data integration have
82 hampered broader adoption and use of this model by a wide range of researchers. Thus, model code
83 may be publicly available, but access to computing resources and the associated technical expertise
84 needed to use them presents barriers to engaging a diverse, cross-disciplinary community of model users
85 who can harness these powerful tools for research and teaching. We contend that broader engagement
86 across scientific disciplines is critical to improving the representation of Earth system processes and their
87 likely responses to global change.

88 This work overcomes some of the barriers to the use of ESMs in ecology by creating an
89 integrated 'NCAR-NEON system'. This system combines meteorological data and site-level ecosystem
90 characterizations from the National Ecological Observatory Network (NEON) with the Community



91 Terrestrial System Model (CTSM), an extension of the Community Land Model (CLM5; Lawrence et al.
 92 2019). CTSM is the terrestrial component of CESM, which is developed with university partners at the
 93 National Center for Atmospheric Research (NCAR; Fig. 1). The NCAR-NEON system also features a
 94 simplified user interface that facilitates access to and use of NEON observations and NCAR models. By
 95 developing this NCAR-NEON system, we aim to enable the convergence of climate and ecological
 96 sciences by providing accessible cyberinfrastructure, quality-controlled datasets from NEON, and tutorials
 97 for analyzing and visualizing observed and simulated data. We describe development of the NCAR-
 98 NEON system, present results comparing observed NEON fluxes with simulations from CTSM, and
 99 outline opportunities that the system enables for research and education across scientific disciplines.



100

101 **Figure 1.** A conceptual diagram illustrating the integration of NEON data and NCAR modeling enabled through the
 102 NCAR-NEON system. NEON meteorological measurements are gap-filled using redundant streams and used as inputs
 103 for single point simulations with the Community Terrestrial Systems Model (CTSM). Additional NEON observations are
 104 used as input data to the model, including surface characteristics of vegetation (e.g., mapping to simulated plant
 105 functional types, PFTs) and the soil properties (soil texture, organic matter content, and depth to bedrock, if < 2m).
 106 Simulations with CTSM are conducted in CESM-Lab, a computing environment that runs in a container or with cloud
 107 computing resources, which includes model code and analysis tools. Simulated data is compared with observed fluxes
 108 using visualization scripts that are provided within CESM-Lab to improve both observed data products, model
 109 parameterization, and model processes representation.

110



111 **2. Methods**

112 **2.1 NEON Data**

113 NEON is a research network comprising 81 monitoring sites (47 terrestrial, 34 aquatic) that are
 114 collecting standardized, open data across the major ecosystems of the United States (Table S1). NEON's
 115 data products are highly complementary to land models, providing high quality and standardized data for
 116 soil, vegetation, and atmosphere states and fluxes across vast spatiotemporal scales with high
 117 throughput instrumented systems data and spatially expansive remote sensing data (Hinckley et al. 2016;
 118 Balch et al. 2020; Durden et al. 2020). Each of the 47 NEON terrestrial sites includes an EC tower to
 119 determine the surface-atmosphere exchange of momentum, heat, water, and CO₂, alongside meteorology
 120 (precipitation, wind speed, humidity, temperature), atmospheric composition (water vapor and CO₂
 121 concentrations and isotopic ratios), and soil sensor assemblies (Metzger et al. 2019). In this preliminary
 122 effort to bring NEON measurements and NCAR modeling together we use NEON data for: 1)
 123 Meteorological inputs that are gap filled and provide local atmospheric boundary condition inputs to
 124 CTSM; 2) Surface characteristics of soil properties and vegetation; and 3) Eddy covariance fluxes to
 125 compare observed and simulated results (Fig. 1, Table 1), with prototype data available through the
 126 NEON data portal (NEON 2023).

128 **Table 1.** NEON data product name, data product use in CTSM, NEON data product ID, and Digital Object
 129 Identifier (DOI). Data products were used for meteorological inputs and surface characterization, which are
 130 inputs needed to run CTSM, and for model evaluation.

Data Product Name	Data Product Use	Data Product ID	DOI
Precipitation	Meteorological input	DP1.00006.001	https://doi.org/10.48443/6wkc-1p05
Relative humidity	Meteorological input	DP1.00098.001	https://doi.org/10.48443/w9nf-k476
Shortwave and longwave radiation (net radiometer)	Meteorological input	DP1.00023.001 *DP1.00024.001 *DP1.00014.001	https://doi.org/10.48443/stbf-bh38 https://doi.org/10.48443/8a01-0677 https://doi.org/10.48443/hv8e-5696
Barometric pressure	Meteorological input	DP1.00004.001 *DP4.00200.001	https://doi.org/10.48443/zr37-0238 https://doi.org/10.48443/7cqp-3j73
Wind speed	Meteorological input	DP4.00200.001 *DP1.00001.001	https://doi.org/10.48443/7cqp-3j73 https://doi.org/10.48443/77n6-eh42
Air temperature	Meteorological input	DP4.00200.001 *DP1.00003.001	https://doi.org/10.48443/7cqp-3j73 https://doi.org/10.48443/q16j-sn13
Forcing height	Meteorological input	DP4.00200.001	https://doi.org/10.48443/7cqp-3j73
Soil physical and chemical properties, Megapit	Surface characterization	DP1.00096.001	https://doi.org/10.48443/10dn-8031
Dominant vegetation type	Surface characterization	Manually Assigned	
Bundled data products - eddy covariance	Model Evaluation	DP4.00200.001 *DP1.00023.001	https://doi.org/10.48443/7cqp-3j73



Net radiation	Model Evaluation	DP1.00023.001 *DP1.00014.001	https://doi.org/10.48443/stbf-bh38 https://doi.org/10.48443/hv8e-5696
Photosynthetically Active Radiation (PAR)	Model Evaluation	DP1.00024.001 *DP1.00023.001 *DP1.00014.001	https://doi.org/10.48443/8a01-0677 https://doi.org/10.48443/stbf-bh38 https://doi.org/10.48443/hv8e-5696
Direct and Diffuse Radiation	Model Evaluation	DP1.00014.001	https://doi.org/10.48443/hv8e-5696
Soil water content and water salinity	Model Evaluation	DP1.00094.001	https://doi.org/10.48443/ghry-qw46

131 *Indicates the data product was used in the redundant stream gap-filling to fill primary data product

132 2.1.1 Meteorological inputs

133 Generating the gap-filled meteorological data that are required for single-point simulations with
 134 land models can be time consuming and requires expertise in micro-meteorology that land model users
 135 and developers may not have. Thus, the modeling community historically relied on external efforts like
 136 FLUXNET synthesis databases to provide gap-fill meteorological measurements at eddy-flux sites (e.g.,
 137 La Thuile or FLUXNET2015; Pastorello et al 2020). Downloading and processing these datasets into a
 138 format that is usable by the model is also time consuming, and often the flux measurements are not
 139 paired with information about local vegetation or soil properties that are easy to discover or digest.
 140 Collectively, these factors create barriers for use and latencies in updating the EC observational data that
 141 are used in single point simulations. The NCAR-NEON system aims to remove some of these barriers.

142 NEON meteorological input data used to run CTSM are summarized in Table 1, and gap-filled
 143 using publicly available code (Table 2). While NEON is highly standardized, a few differences in
 144 instrumentation exist between NEON Core (representative of the predominant natural ecosystem of each
 145 respective Domain) and gradient sites (representing other endmember conditions in each respective
 146 Domain). For example, core NEON sites measure precipitation with Double-fenced Intercomparison
 147 Reference gauges, while gradient sites all have tipping buckets (Metzger et al. 2019). Accounting for
 148 these site-specific sensor configurations and variation in their associated data streams is the first step in
 149 providing usable meteorological inputs to CTSM. The meteorological inputs to CTSM must be continuous,
 150 therefore, additional gap filling of missing data is required. Additionally, the EC system collects data
 151 necessary to calculate fluxes of energy, water vapor, and CO₂. The NEON site design builds in some
 152 redundancy in observations with profiles of incoming radiation, wind, temperature, water vapor, and CO₂
 153 concentrations measured at different heights on each NEON tower (Metzger et al. 2019). These data
 154 redundancies allow for a robust initial gap-filling using linear regressions among the primary and
 155 redundant data streams to correct for instrument or location differences. For example, if wind speed or air
 156 pressure measurements from the tower top are missing, we gap-fill with the value from the redundant
 157 data stream (typically measured at a lower tower height) corrected by the linear relationship with the
 158 primary sensor data. If multiple redundant data streams are available, the best fit regression with data
 159 available is used to determine the gap-filled value for each missing data point.



160 After gap-filling using related data stream regression, some range thresholds and proper unit
161 conversions are applied to prepare the meteorological data for processing through the ReddyProc R
162 package following the gap-filling workflow outlined in Wutzler et al. (2018). After using related data stream
163 regressions, the meteorological data are checked for additional gaps, and gap-filling is performed using
164 one of three additional gap-filling methodologies that include look-up table (Falge et al. 2001), mean
165 diurnal course, and marginal distribution sampling (Moffat et al. 2007; Reichstein et al. 2005). The gap-
166 filling method is tracked and provided as a flag with the data to allow users to assess data with various
167 methodology restrictions. The meteorological data streams are then converted to units required by CTSM
168 and output to cloud storage in netCDF format with associated metadata to fully describe data provenance
169 and formatting. At most sites data coverage spans January 1, 2018, through December 31, 2021, but as
170 more NEON data are collected these files will also be updated in near-real time, thus removing barriers
171 associated with processing flux tower data and reducing latencies in using new data as they are
172 collected. Tables S1 and S2 provides a list of all the sites where input data have been successfully gap-
173 filled and notes any potential data quality issues.
174



175 **Table 2** List of helpful websites created for the NCAR-NEON system, their contents and a url address for each. All sites
 176 were accessed Feb 13, 2023. *Note we intend to provide permanent urls for these sites in the final published
 177 manuscript.

Name	contents	url
Project home page	Main landing page for users interested in learning more about the project	https://ncar.github.io/NEON-visualization/
Tutorial	Tutorial that introduces running CTSM at NEON tower sites in the CESM-Lab container.	https://ncar.github.io/ncar-neon-books/notebooks/NEON_Simulation_Tutorial.html
Interactive visualizations	Interactive plots that allow users to explore data produced by the NCAR-NEON system without running the model or downloading data.	https://neon.herokuapp.com/neon_dashboard
Processing NEON data	Docker image with scripts used for gap filling meteorological data, flux partitioning, and formatting NEON datasets.	https://quay.io/repository/ddurden/ncar-neon
DiscussCESM Forum	Discussion forum bulletin boards for questions related to CESM including CESM-Lab and CTSM.	https://bb.cgd.ucar.edu/cesm/
CTSM repository	Code base, technical documentation and information related to CTSM	https://github.com/ESCOMP/CTSM
NEON Prototype Data	NEON prototype datasets, which include the gap filled meteorological data for flux partitioned data used for model input and evaluations	https://data.neonscience.org/prototype-datasets/0a56e076-401e-2e0b-97d2-f986e9264a30

178

179



180 *2.1.2. Surface characteristics of soil properties and vegetation*

181 Basic information on edaphic properties is needed in the pedotransfer functions that describe soil
182 thermal and hydraulic properties in CTSM. Although NEON has several soil sampling datasets, we used
183 information from the Megapit characterization of soil physical and chemical properties in CTSM because it
184 contains more information about deep soil horizons (> 1 m depth; Table 1) from a single soil pit at each
185 site. Megapit samples were collected by pedogenic soil horizon down to 2 m or restrictive feature and
186 analyzed for several properties including total soil carbon concentration, calcium carbonate concentration,
187 bulk density, coarse fragments, soil pH, and texture. Soil organic carbon stocks used in CTSM were
188 estimated for each soil horizon by calculating organic carbon concentrations (after subtracting carbonates
189 from total carbon measurements) and multiplying by bulk density.

190 Currently, the CTSM simulations are run with a single plant functional type (PFT) at each NEON
191 site (Table S1). We acknowledge that this belies the diversity in vegetation that is present at NEON sites,
192 but it provides a tractable starting point for further investigation into developing more sophisticated site-
193 regional-scale parameterizations and representations of biotic diversity with CTSM. The dominant PFT at
194 each NEON site was assigned at the location of each EC tower using expert assessment that was
195 informed by NEON vegetation surveys. Information on soil properties and dominant vegetation types are
196 output as .csv files to public-access cloud storage buckets for use by CTSM (Figs. 1; Sect. 2.3).

197 *2.1.3 Independent model evaluation*

198 The EC flux data (energy, water vapor, and CO₂) are time regularized and quality assurance and
199 control (QA/QC) are applied. The QA/QC applied includes removing data when quality flags are raised,
200 removing CO₂ data when the field calibration algorithm cannot be applied, applying range thresholds, and
201 applying a despiking routine to remove outliers (Brock, 1986; Starkenburg et al. 2016). The data are gap-
202 filled using the ReddyProc methodology outlined in Sect. 2.1.1. The vapor pressure deficit (VPD) is
203 derived from the difference between actual and saturated vapor pressure, while gross primary production
204 (GPP) is calculated from net ecosystem exchange (NEE) using the nighttime flux partitioning method of
205 Reichstein et al. (2005). The data, quality flags, and metadata are formatted and provided at 30-minute
206 intervals as netCDF files for comparison with modeled fluxes. Finally, NEON continuous soil moisture
207 data were compared with model simulations for two sites. Since the soil moisture sensors were
208 reconfigured with different calibration coefficients during the 2018-2021 validation period, which
209 introduced step changes in NEON's soil moisture data product (Table 1), the raw sensor measurements
210 were back-calculated and consistent soil-specific calibration coefficients were subsequently applied over
211 the entire measurement period (Ayres et al. 2021) prior to comparison with CTSM data. Only values that
212 passed quality tests were used. In future work we aim to provide standardized soil moisture data for more
213 sites across the Observatory.



214 **2.2. NCAR modeling**

215 Numerical models of weather and climate have long been recognized as essential research tools
216 to advance atmospheric science. Land surface fluxes of energy, moisture, and momentum, required to
217 solve the equations of atmospheric physics and dynamics, are controlled by heat and water storage in
218 soil, as well as the physiology of plants and their organization into canopies of leaves. Consequently,
219 models of soil-plant-atmosphere processes are required to provide the necessary surface fluxes. Indeed,
220 the first numerical weather prediction model included mathematical equations for soil temperature, soil
221 moisture, the stomata on leaves, and envisioned canopies as a film of leaves covering the surface
222 (Richardson 1922). As science progressed from models of atmospheric general circulation to climate
223 models and now, Earth system models, the role of terrestrial ecosystems in climate processes has come
224 to the forefront. The terrestrial components of ESMs, such as CTSM, have improved ecological processes
225 representation and now include biogeochemical cycles, wildfires, and land use and land cover change
226 (Bonan 2015, 2019; Lawrence et al. 2019). This evolution in the Earth system sciences is evident in 40+
227 years of scientific research linking weather, climate, and land modeling at NCAR, from pioneering initial
228 model implementations (Deardorff 1978; Dickinson et al. 1986, 1993; Bonan 1996) to community-based
229 model development (Oleson et al. 2004, 2010, 2013; Levis et al. 2004; Lawrence et al. 2019) that
230 continues to engage ecological and environmental sciences communities in CTSM development and
231 application. As more ecology and biogeochemistry are added to the models (Fisher and Koven, 2020),
232 the notion of climate prediction is expanding to Earth system prediction, including terrestrial ecosystems
233 and biotic resources (Bonan and Doney 2018). These models have also become important tools for
234 scientific discovery by identifying the ecological processes that affect climate (e.g., photosynthetic
235 temperature acclimation; Lombardozzi et al. 2015) and to advance theory at the macroscale (e.g.,
236 developing a theory of ecoclimatic teleconnections; Swann et al. 2018). With the new NCAR-NEON
237 system tools described here, we aim to expand engagement and accessibility with the ecological and
238 environmental sciences communities to continue testing, evaluating, and improving terrestrial process
239 representation within CTSM. This will improve our understand of how ecosystems function within the
240 Earth system, including the regulation of carbon, water, and energy fluxes that affect climate.

241 *2.2.1 Containerized version of CESM-Lab*

242 CESM has a long history of being freely and openly available to users (Hurrell et al. 2013;
243 Danabasoglu et al. 2020), yet several barriers related to training, cyberinfrastructure, and data integration
244 have hampered its adoption by a wide range of researchers. Even with open-source software, porting
245 CESM to a new computer also requires the new computing system can compile model source code and
246 has all the necessary input data and library dependencies. To address these computing challenges,
247 NCAR recently developed CESM-Lab, which is a pre-configured and standardized environment that
248 contains CESM and Jupyter-Lab. CESM-Lab is available via a Docker container and distributed via
249 DockerHub (Table 2). The containerized version of CESM-Lab, and containers in general, give



250 researchers the capability to package and distribute source code, libraries, dependencies, and system
251 settings as one unit – thereby ensuring reproducibility. Using the containerized system, CESM-Lab can
252 be used on any computing system, even a laptop or a cloud platform, to allow researchers to easily run
253 CESM and its component models. The NCAR-NEON system uses CESM-Lab capabilities to run single
254 point CTSM simulations at NEON sites.

255 *2.2.2 Single point CTSM simulations*

256 The workflow for running single-point CTSM simulations requires several steps that can be error-
257 prone and time-consuming, particularly when using EC tower or other site-level data to drive simulations.
258 To facilitate using NEON data in CTSM simulations we made several modifications to simplify this
259 workflow. When users create a new simulation, the system queries NEON public-access cloud storage
260 buckets and downloads available data into a designated directory (Sect. 2.3). For each NEON site, this
261 includes a surface dataset that reflects soil properties and the dominant vegetation (Table 1),
262 meteorological data used to drive the atmospheric conditions, and an initial conditions file with
263 equilibrated carbon, water, energy, and nitrogen states and fluxes. Initial conditions at each NEON site
264 were generated by cycling over the meteorological data at each site for 200 years in accelerated
265 decomposition (AD) mode and another 100 years in normal, or post-AD mode, or until biogeochemical
266 states reached steady state (when ecosystem C pools change by $< 1\text{ g C m}^{-2}\text{ y}^{-1}$; this is standard protocol
267 for equilibrating the model state, Lawrence et al. 2019). Colder sites, especially those in Alaska, took
268 longer to reach these steady state conditions.

269 The NCAR-NEON system uses a top-level Python code called 'run_neon' that simplifies
270 downloading the preconfigured datasets and automatically creates, builds, and runs cases for individual
271 and multiple NEON sites. The Python script, which also resides in the CTSM repository (Table 2),
272 includes several command-line arguments and options for automatically running spin-up and transient
273 simulations. Collectively, these features dramatically improve CTSM site simulation accessibility, facilitate
274 the use of new NEON data, reduce potential errors in configuring the CTSM case at NEON tower sites,
275 and enable users to run simulations at multiple NEON sites. While users of the system can now easily
276 generate their own data, NCAR provides model simulation data at each of the tower sites that are
277 available on the NEON public-access cloud storage bucket (Sect. 2.3). Simulation data are generated at
278 a 30-minute time step and are aggregated into daily netCDF files.

279 *2.2.3 Tutorials, analysis, and visualization*

280 Three interactive tutorials are available to guide users through the new NCAR-NEON system
281 (Table 2). The first tutorial helps system users to access CESM-Lab using Docker, which will ultimately
282 allow the user to run CTSM simulations at NEON sites on their local computing system. The first step
283 requires that users download Docker from the company website. This step is potentially challenging, as
284 Docker is an externally controlled application and some recent Docker updates do not work with older



285 computing systems. We provide links to additional resources to help the user navigate these potential
286 problems and offer a resource for asking questions about containers through the CESM discussion forum
287 (Table 2). After downloading and installing Docker, users are guided through downloading, running, and
288 connecting to the CESM-Lab container and accessing the NEON tower simulation and visualization
289 tutorials.

290 The second tutorial is a Jupyter Notebook that guides users through running CTSM simulations
291 for NEON flux tower sites. The beginning of this tutorial provides a short description about CTSM and its
292 component models, as well as resources for finding additional information. The process of running a
293 simulation at NEON tower sites has been streamlined into the 'run_neon' script (see Sect. 2.2.2) that can
294 be called with a single line of code after the user defines a NEON tower site. The simulation itself
295 downloads approximately 2.5 GB of input data and takes several minutes or more to complete, depending
296 on the speed of the internet connection and computing system being used. After the simulation
297 completes, the user is pointed to where the model data are stored and has the option to generate plots of
298 soil temperature and moisture profiles for one year of the simulation.

299 The third tutorial guides users through analyzing and evaluating model simulations against
300 observed NEON flux tower measurements. This tutorial requires a successfully completed NEON tower
301 simulation from the previous simulation tutorial. The user selects their site and the year of interest and is
302 guided through loading and opening the model data files, as well as downloading EC data for evaluation
303 from the NEON server and loading and opening the files. Next, the tutorial guides users through
304 formatting, processing, and plotting simulation and flux tower data. Users generate plots of mean annual
305 and diel cycles of latent heat flux. Additional plots illustrate how CTSM partitions latent heat flux into
306 ground evaporation, canopy evaporation, and transpiration, as component fluxes are not available from
307 the observed data. Scatter plots are also created using simulated fluxes to illustrate the relationship
308 between component evaporation and transpiration fluxes and total latent heat flux on seasonal and
309 annual timescales. The tutorial explains the python tools used to process and plot the data and asks
310 probing questions about the results that tutorial users are exploring to help guide the user in thinking
311 about patterns in the data and consider how to compare model and flux tower data. Users are
312 encouraged to use the code available in this tutorial to explore other sites, years, and variables.

313 **2.3 Cyberinfrastructure to Facilitate Data Exchange and Interactive Visualizations**

314 Cyberinfrastructure for scientific data provides data handling and management functionality
315 including data storage, processing, transfer, security, and access. Cyberinfrastructure components
316 developed for the NCAR-NEON system include access-managed cloud storage for project data,
317 standards-based metadata generation enabling dataset search and discovery, and data exploration tools
318 for the user community. Datasets for the NCAR-NEON system are hosted in cloud object storage
319 providing secure web-enabled access to the data files (Fig. 2). Data files are grouped in the cloud storage
320 system into logical storage containers called buckets. Buckets that are granted public access allow

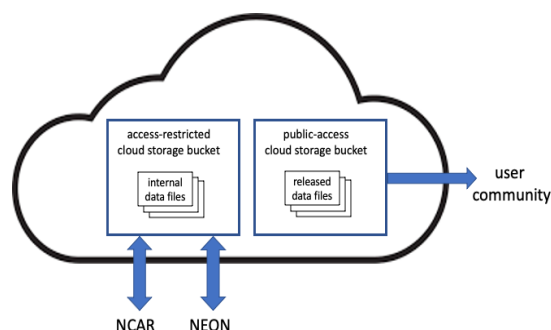


Figure 2. A schematic representation of the cloud-based data management for the NCAR-NEON system. Internal data may include preliminary results, data shared for review within the project, or data staged for release. Released data files are available for public access to the user community and anyone on the Internet and include NEON meteorological inputs, NEON surface characterization data, CTSM surface datasets and initial condition files, NEON measurements used for model evaluation, and data from CTSM simulations that are used for interactive visualizations. Access-restricted cloud buckets require authentication to access files stored in them. Public-access cloud storage buckets provide open access to the files stored in them.

anyone on the Internet to download the data stored in them. Buckets protected with authentication mechanisms require users to have either individual account permissions on the bucket or an access key for the bucket and are meant for internal dataset sharing or staging data prior to public release.

Data exchange between NCAR and NEON within this system enables automated generation of datasets as well as collation of NCAR model outputs and NEON data. The initial data collation for NEON data products uses a container that sources all atmospheric forcing and model evaluation data from the NEON API, performs gap-filling, and formats the data for model ingestion with standardized metadata (Sect. 2.1). Simulation datasets from NCAR (Sect. 2.2) are

339 automatically synced to NEON object storage in the cloud at scheduled intervals (Fig. 2). To facilitate
 340 automated transfer of datasets between NCAR and NEON, a staging bucket is configured that allows file
 341 uploads from authenticated users. An automated process moves files from the staging bucket to the
 342 publicly available target bucket at scheduled intervals. Metadata describing scientific datasets using
 343 standard vocabularies and formatting can be used by Internet search engines to facilitate dataset
 344 discovery. JavaScript Object Notation for Linked Data (JSON-LD; <https://www.w3.org/TR/json-ld>) is a
 345 human- and machine-readable open metadata standard. Schema.org defines a vocabulary of standard
 346 HTML tags compatible with JSON-LD markup (Shepherd et al. 2022). A metadata generation component
 347 for NCAR-NEON datasets is implemented in Python and uses the Binary Array Linked Data library
 348 (binary-array-ld 2016) to generate JSON-LD metadata for NCAR-NEON netCDF files with the
 349 Schema.org vocabulary.

350 Beyond these automated data exchanges, we also developed a Python-based interactive
 351 visualization dashboard (Table 2) as a Graphical User Interface (GUI) that enables users to explore and
 352 interact with model outputs and observations on-the-fly. This tool allows users to generate graphs and
 353 statistical summaries comparing CTSM simulations and observational data for NEON sites without
 354 downloading the observational data or running the model. This dashboard was developed using a
 355 scientific Python stack, including Xarray, Bokeh, and Holoviews, which allows a developer to create a
 356 user interface with widgets and visualization components inside a Jupyter Notebook. Users access a GUI
 357 to select individual NEON sites, variables, and output frequencies to visualize. The tool offers different



358 types of interactive visualizations and statistical summaries based on users' selections. This interactive
359 visualization dashboard does not require specialist knowledge to operate; therefore, it can be used for
360 educational outreach activities and in classrooms. Moreover, users can interact with the dashboard using
361 a browser, so it is possible to interact with the plots via tablet or smartphone.

362 Data I/O and manipulation, particularly at the 30-minute frequency available in the NCAR-NEON
363 system, are typically computationally resource-intensive aspects of data access. I/O and calculations can
364 both benefit from parallel computing, which can process multiple subsets of a dataset simultaneously and
365 thereby enable efficient dataset access and operations. The back end for the visualization dashboard
366 uses dataset chunking for efficient access to netCDF file content. The Zarr format and library enable
367 generation of metadata providing chunked access to netCDF files (Miles et al. 2022). Zarr metadata for
368 daily files is combined into monthly files, reducing the number of files accessed for time intervals
369 spanning multiple days and thereby improving access efficiency. The Python Xarray library, which is used
370 to read the datasets, integrates with the Python Dask library for parallel computing and thus enables
371 loading and processing netCDF data chunks in parallel as Dask arrays. The Dask components that
372 Xarray uses use a local thread pool by default, and local threads incur minimal task overhead associated
373 with the parallel processing. Operations on the Dask arrays use the Python NumPy library for array
374 operations, and the NumPy implementation takes advantage of thread pool parallelism, enabling
375 efficiency improvements in dataset operations even on small (~100-200 KB) files.

376 **3. Results**

377 We illustrate features of the NCAR-NEON system with comparisons of observed and simulated
378 fluxes across diverse ecosystems that the Observatory spans. A subset of the sites highlighted in our
379 analysis are described in Table 3. The comparisons are intended to summarize the status of the project,
380 illustrate the data produced through this project, and highlight potential insights the data affords. We
381 recognize that there are rich opportunities to expand on these analyses, integrate additional
382 measurements, and improve modeled parameterization and representations of specific sites and
383 processes. Indeed, such contributions are encouraged from the community.

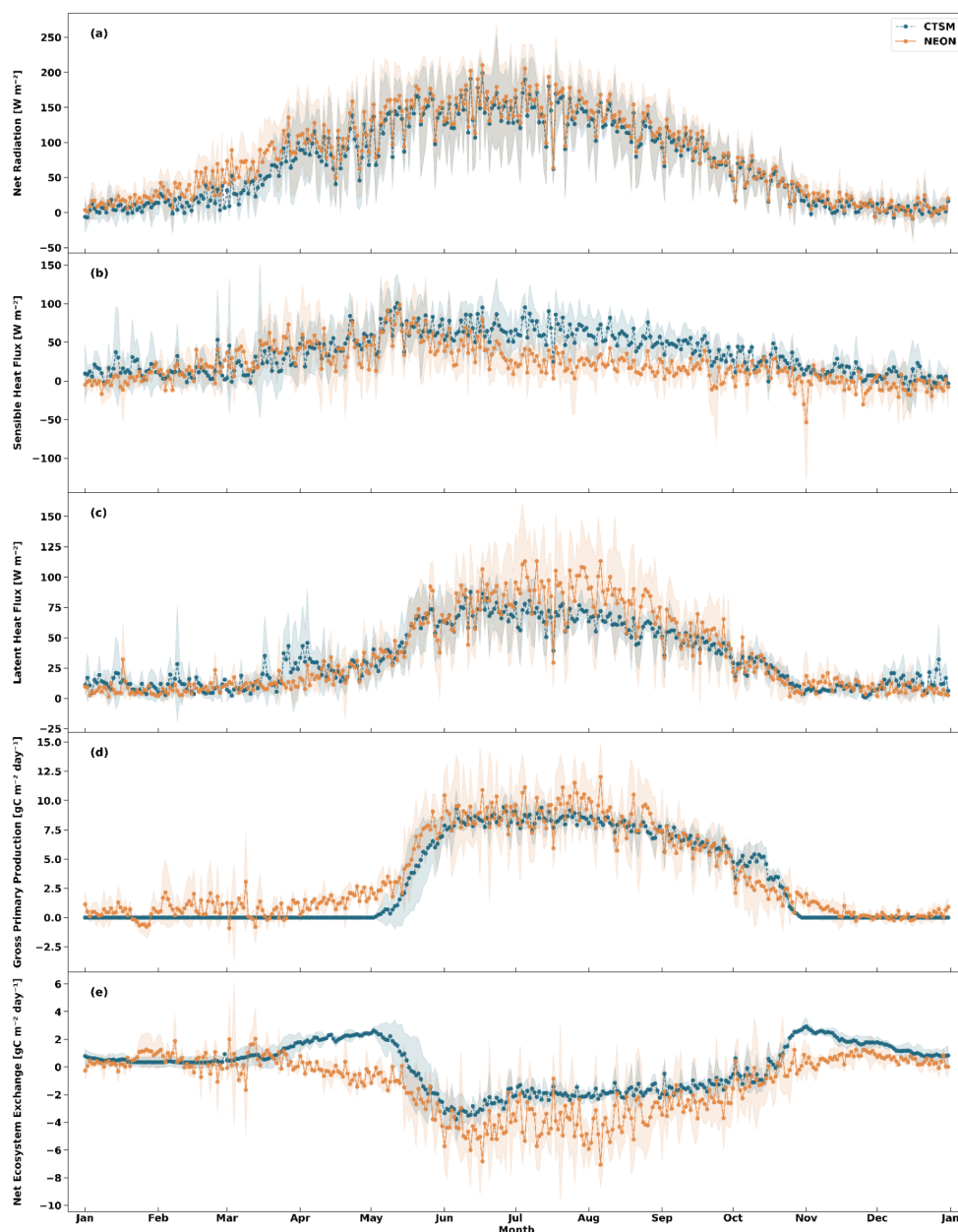
384



385 **Table 3** Summary of site name, location, mean annual temperature (MAT), mean annual precipitation (MAP), and gross
 386 primary production (GPP) at a subset of NEON sites. Due to gaps in the observational estimates, mean annual GPP is
 387 for the full time series simulated by CTSM at each NEON site. All results are for 2018-2021 unless noted otherwise.
 388 The full list of results is shown in Tables S1, S2.

NEON Site ID	Site Name	Lat	Lon	MAT (°C)	MAP (mm y ⁻¹)	GPP (gC m ⁻² y ⁻¹)
BART	Bartlett Experimental Forest	44.06516	-71.28834	7.7	1213	1127
HARV	Harvard Forest	42.53562	-72.17562	8.5	1405	1153
STEI	Steigerwaldt-Chequamegon	45.5076	-89.5888	5.7	660	1109
KONZ	Konza Prairie Biological Station	39.1007	-96.56227	12.9	617	1158
SRER	Santa Rita Experimental Range	31.91068	-110.83549	20.4	329	360
ABBY	Abby Road	45.762378	-122.329672	10.1	2043	1906

389 Annual climatologies of site level data provide comparisons of measured and simulated fluxes.
 390 Site level simulations with CTSM received inputs of incoming shortwave and longwave radiation
 391 measured at NEON EC towers (Table 1), but the model calculates reflected shortwave radiation and
 392 outgoing longwave radiation based on albedo and surface temperature. Accordingly, net radiation is a
 393 useful metric by which to compare observed and simulated fluxes. Since net radiation is a driver of
 394 numerous ecosystem fluxes, identifying biases can help to explain biases in other fluxes. We look at a
 395 climatology of daily mean net radiation that is simulated over the NEON record. Results shown here for
 396 Bartlett Experimental Forest (BART; Fig. 3a) suggest that the model adequately captures the seasonal
 397 cycle of net radiation at this temperate deciduous forest site. (Fig. S1 shows a similar climatology for a
 398 boreal forest site at DEJU).
 399



400
 401 **Figure 3** Climatology of daily mean NEON measurements (orange) and CTSM simulations (blue) at the Bartlett
 402 Experimental Forest in New Hampshire (BART). Points show the daily mean (a) net radiation; (b) sensible heat flux;
 403 (c) latent heat flux; (d) gross primary production (GPP); and (e) net ecosystem exchange (NEE). Shading shows the
 404 standard deviation of daily average data for 2018-2021.

405

406 Users can also compare latent and sensible heat fluxes that are simulated by the model and
 407 observed at EC towers. At BART we see that CTSM tends to underestimate sensible heat fluxes, while



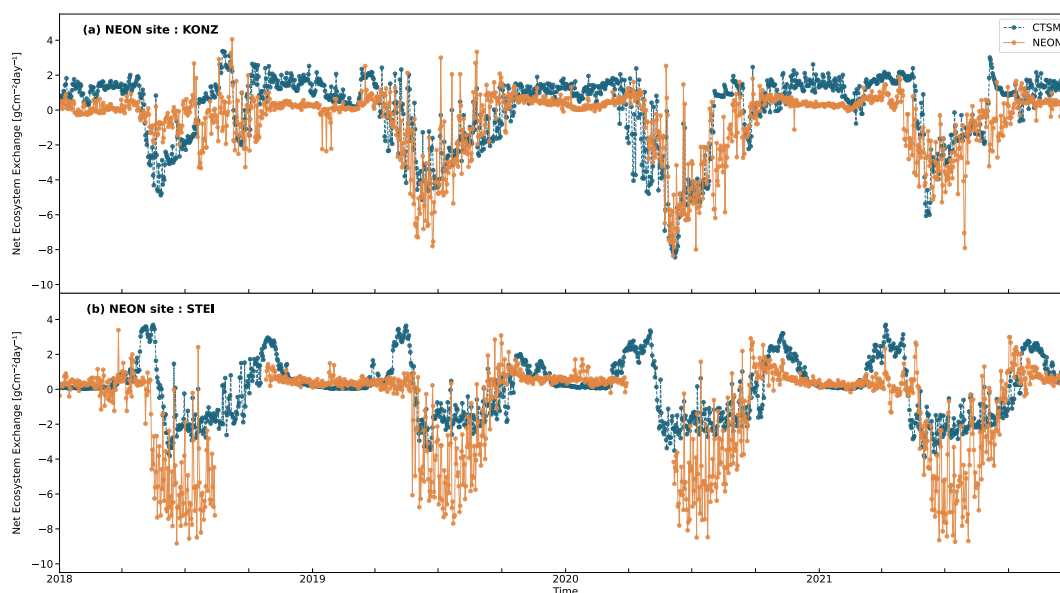
408 overestimating latent heat fluxes, especially during the summer months (Fig. 3b-c). Such biases in the
409 evaporative fraction (the ratio of latent heat flux to the sum of latent and sensible heat fluxes) of turbulent
410 fluxes are common in land models, including CTSM (Best et al. 2015; Wieder et al. 2017) and the NCAR-
411 NEON system. The inconsistencies at BART could reflect model biases in stomatal conductance or leaf
412 area index (LAI) and deserves further investigation. Future work can leverage data from PhenoCam data
413 (Richardson et al. 2018) and stable isotope measurements at NEON towers (Finkenbiner et al. 2022;
414 Moon et al. 2022) to better understand LAI and stomatal conductance, respectively.

415 Comparing measured and simulated carbon fluxes provides insights into model parameterizations
416 and can be used to estimate missing observational data. Carbon fluxes from CTSM simulations can be
417 compared to data from NEON EC towers: Net ecosystem exchange (NEE) data are measured at the
418 NEON EC towers while GPP is a modeled product that is derived from statistical relationships, here using
419 the nighttime flux partitioning method of Reichstein et al. (2005). By contrast, models like CTSM first
420 simulate GPP based on leaf level photosynthetic rates that are scaled to the canopy with simulated LAI.
421 Subsequently, NEE is calculated after subtracting ecosystem respiration fluxes from GPP. Results at
422 BART suggest that CTSM generally captures the timing and magnitude of GPP fluxes at the site (Fig. 3d);
423 although attention to phenology, especially environmental controls and interannual variability of leaf out
424 and senescence are likely warranted (Birch et al. 2021; Li et al. 2022). The climatology of NEE fluxes
425 simulated by CTSM shows biases during the spring and autumn when the model simulated a land source
426 of CO₂ to the atmosphere (Fig. 3e) due to high ecosystem respiration fluxes. Moreover, the land sink of
427 CO₂ in the summer appears to be weaker in CTSM simulations than the NEON observations at the BART
428 tower (Fig. 3e). Since the magnitude of GPP is similar in the model and observations, the underestimated
429 summer NEE is possibly due related to high biases in simulated ecosystem respiration fluxes. Diagnosing
430 the source of this model biases is challenging, in part due to the interconnectivity of simulated processes
431 and the limited capacity to measure such processes. Deeper insights may be afforded by taking a closer
432 look at results with higher temporal frequencies.

433 NEON tower data are simulated in near-real time within the NCAR-NEON system, with data
434 available to simulate most towers starting in 2018 through the most recent full year, here 2021. Figure 4
435 shows daily mean carbon fluxes, NEE, that are measured and simulated for the Konza Prairie Biological
436 Station (KONZ), where the NEON tower is in an unplowed tallgrass prairie in Kansas, and Steigerwaldt
437 Land Services (STEI) site, where the NEON tower is located in an early successional aspen stand in
438 Wisconsin. Positive NEE fluxes show net carbon release from land to the atmosphere, while negative
439 fluxes indicate carbon gain into ecosystems. Looking at the full data record shows several notable
440 features of NEON measurements and CTSM simulations. Data gaps in NEON measurements are most
441 common during the early operation of the observatory (Aug-Oct of 2018 at STEI) and in the early months
442 of the COVID-19 pandemic, when field crews could not travel to field sites to maintain equipment (Apr-
443 June of 2020 at STEI). Across the observatory the NEON EC measurements have greater than 70% data
444 coverage, up from less than 40% data coverage at the start of observatory operations. The current NEON



445 EC data coverage aligns with that of the FLUXNET2015 dataset (van der Horst 2019). Second, although
 446 EC is directly measuring NEE, mean daily NEON observations show high variability at both sites. Finally,
 447 NEON EC towers measure both storage and turbulent fluxes, but results shown here omit the storage
 448 component. Storage fluxes contribute to uncertainty in measured NEE fluxes, which may (or not) be large
 449 for individual sites at different times of year.
 450



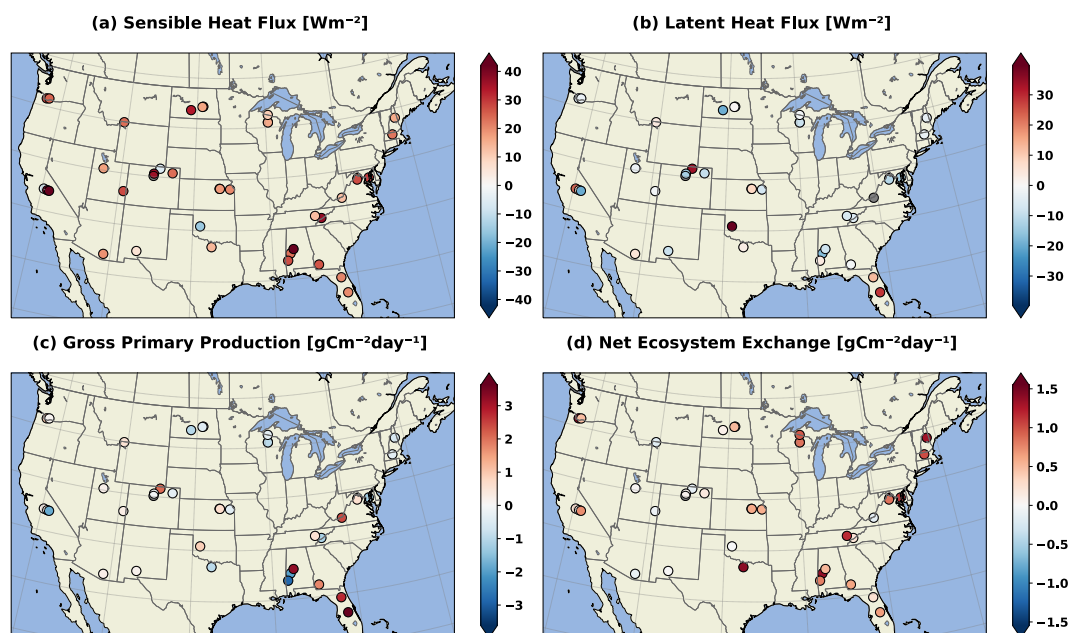
451
 452 **Figure 4** Full time series of daily mean net ecosystem exchange (NEE) from NEON measurements (orange) and CTSM
 453 simulations (blue) at the (a) Konza Prairie Biological Station in Kansas (KONZ) and (b) Steigerwaldt Land Services site
 454 in Wisconsin (STEI). Positive NEE fluxes show net carbon release from land to the atmosphere, while negative fluxes
 455 indicate carbon gain into ecosystems.

456
 457 The NEE fluxes that are simulated by CTSM are calculated as the differences in GPP and
 458 ecosystem respiration fluxes, which includes both autotrophic and heterotrophic respiration. These
 459 component fluxes are much larger, depend on simulated ecosystem states (LAI, vegetation biomass, and
 460 soil organic carbon stocks) and have associated environmental sensitivities (e.g., temperature,
 461 precipitation, etc.). Thus, biases in these component fluxes can potentially transmit biases to simulated
 462 NEE fluxes (Figs. 3-4). For example, CTSM simulations show periods of positive NEE during the spring
 463 and fall that are not evident in NEON observations. The seasonal biases in NEE could result from an
 464 underestimation of GPP during the shoulder season caused by phenological mismatches in simulated
 465 and observed LAI, or result from only simulating a single plant functional type in CTSM. Alternatively,
 466 NEE biases could result from higher than observed soil respiration rates in the model that reflect potential
 467 biases in total soil C stocks or the temperature sensitivity of heterotrophic respiration. Finally, the CTSM
 468 simulations were equilibrated to steady state conditions, meaning that annual NEE averaged over the
 469 simulation period will be zero. The real ecosystems being measured at NEON sites, however, have



470 historical legacies – KONZ is burned periodically and STEI is an aggrading forest site – and do not
 471 necessarily meet these same steady state assumptions. Collectively, this points to rich opportunities to
 472 learn about the ecosystems being measured by NEON observations and the processes that are important
 473 to represent in models like CTSM.

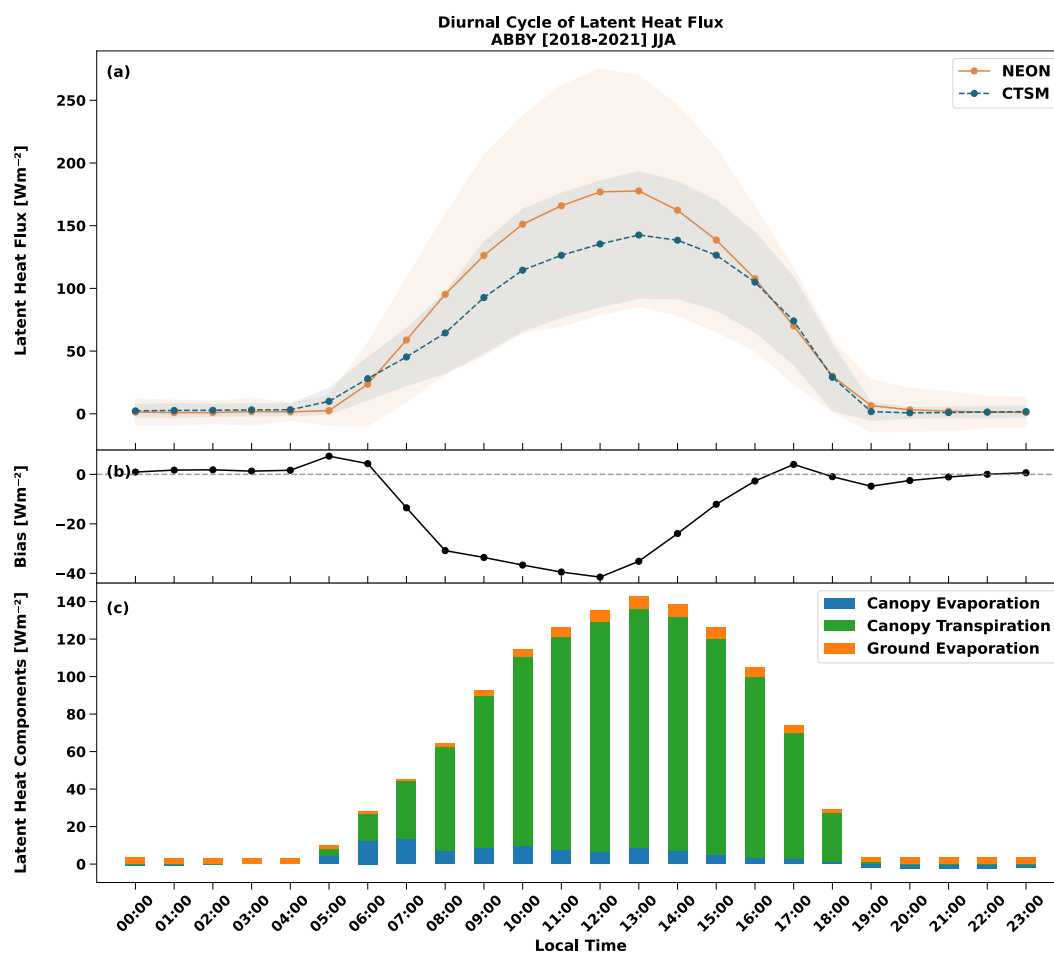
474 We calculated summary statistics of CTSM simulated bias (Fig. 5) and root mean square error
 475 (RMSE; Fig. S2) in ecosystem fluxes, compared to NEON observations. Biases in GPP and NEE are
 476 relatively low in the Great Plains and Intermountain West but are larger in the Eastern US. Specifically,
 477 NEE is biased high east of the Mississippi, while GPP biases are largest in the Southeastern US. CTSM
 478 typically has high biases in sensible heat fluxes and concurrent low biases in latent heat flux. Some sites,
 479 particularly grasslands (e.g., CPER, OAES, and SJER), do not follow this general pattern. We therefore
 480 probed precipitation data from NEON, which appear to have significant biases at some grassland sites
 481 (discussed in Sect. 4.1) and contribute to artificially high biases in CTSM simulations at these sites.
 482



483
 484 **Figure 5** Maps showing location of NEON site in the conterminous United States and annual biases in fluxes that are
 485 simulated by CTSM for: (a) sensible heat flux ($W m^{-2}$); (b) latent heat flux ($W m^{-2}$); (c) gross primary production (GPP,
 486 $gC m^{-2} day^{-1}$); and net ecosystem exchange (NEE, $gC m^{-2} day^{-1}$) over the observational record (2018-2021), unless
 487 otherwise noted in Table S2.

488

489 Additional insights into potential sources of biases in data-model comparisons can be provided by
 490 looking deeper into component fluxes of latent heat at higher temporal frequencies. The NEON EC towers
 491 provide 30-minute measurements of total latent heat fluxes, but latent heat fluxes in CTSM can be
 492 partitioned into contributions from canopy transpiration, canopy evaporation, and soil evaporation. For



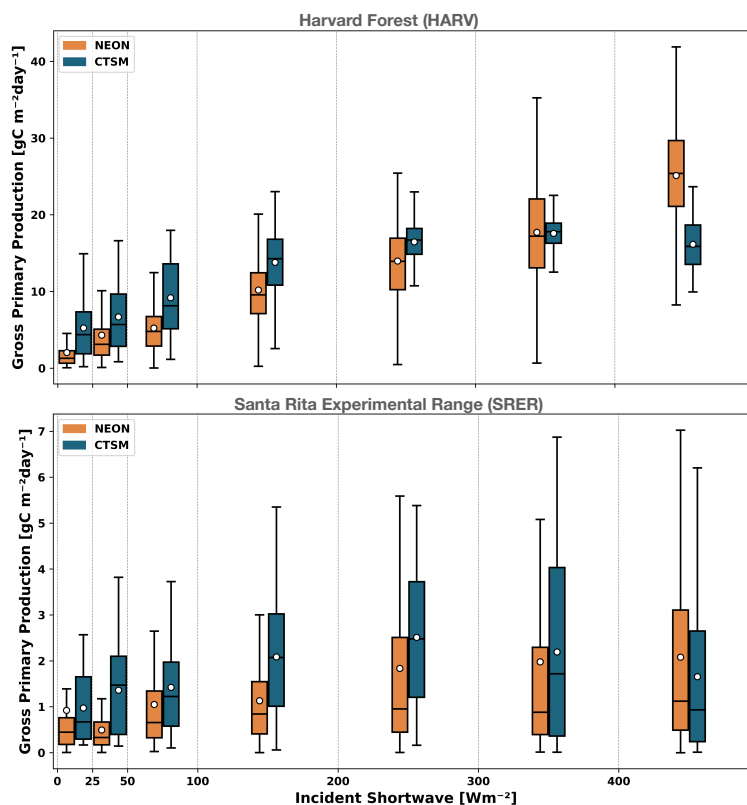
493
 494 **Figure 6** Diel cycle of summertime (June, July, and August, or JJA) latent heat flux at the Abby Road site in Washington
 495 (ABBY). Panels show: (a) mean half hourly fluxes (2018-2021 mean $\pm 1\sigma$) for NEON measurements and CTSM
 496 simulations (orange and blue lines, respectively); (b) CTSM model bias relative to the observations ($W m^{-2}$); and (c)
 497 partitioning of latent heat into fluxes that are simulated by CTSM, which includes canopy evaporation, canopy
 498 transpiration, and ground evaporation (blue, green, and orange bars, respectively). Additional visualizations showing
 499 all sites and seasons are available on the interactive visualizations web site (Table 2).

500

501 example, the CTSM simulations show temporal biases in both the timing and magnitude of mean diel
 502 cycle of summertime (June, July, and August, or JJA) latent heat fluxes at the NEON Abby Road site
 503 (ABBY; Fig. 6). The bulk of daytime latent heat fluxes simulated by the model are coming from canopy
 504 transpiration fluxes, suggesting that the representation of stomatal conductance does not respond
 505 correctly to atmospheric conditions or plant water availability. We also note that this site experienced two
 506 very strong heatwaves in the summers of 2020 and 2021. Additional measurements of soil moisture, LAI,
 507 or sap flux could help test, evaluate, and improve various model parameter values and parameterizations
 508 to produce results that are most consistent with observed fluxes.



509 Light response curves (Fig. 7) illustrate how canopy photosynthesis responds to changes in the
 510 radiation environment. At forested sites, CTSM tends to overestimate GPP at low light levels,
 511 underestimate GPP under full irradiance and simulate lower variance in GPP across a range of high
 512 incident radiation; this pattern is illustrated in Fig. 7a for Harvard Forest. At the Santa Rita grassland site,
 513 GPP is biased high in most irradiance bins, although is comparable to observed estimates of GPP at full
 514 irradiance (Fig. 7b). As GPP is the driver for carbon fluxes and plant-mediated water fluxes in CTSM,
 515 inaccurate responses to light environment affects several processes, including NEE and transpiration,
 516 which is a primary driver of mid-day (Fig. 6c) and summertime latent heat flux.
 517

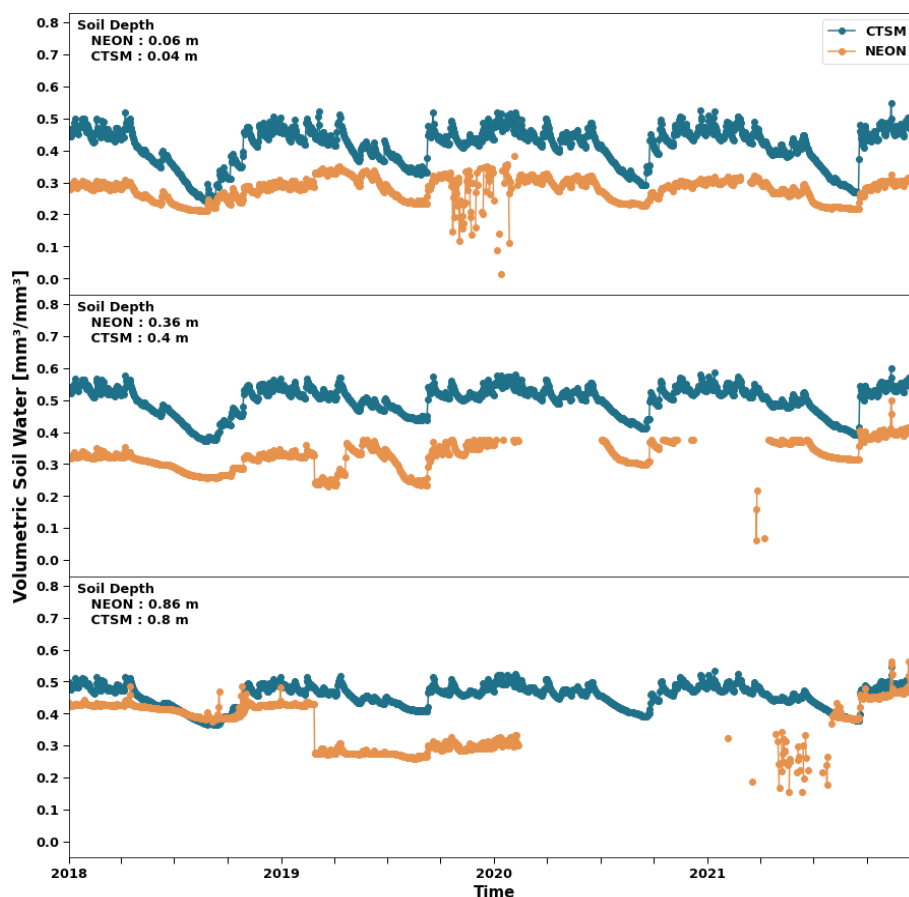


518
 519 **Figure 7** Box-whisker plots showing light response curves, the relationship between gross primary production (GPP)
 520 and incident shortwave radiation, that are derived from NEON measurements and CTSM simulations (orange and blue,
 521 respectively) at (a) Harvard Forest (HARV) and the (b) Santa Rita Experimental Range (SRER). Data represent 30-
 522 minute measurements that are binned by incident shortwave radiation levels observed at NEON sites over the
 523 observational record in July (2018-2021). Boxes show the mean (dots), median (line), interquartile range (boxes). The
 524 whiskers extend from the boxes (showing first and third quartiles) by 1.5 times the interquartile range (Q3-Q1). Note
 525 differences in the scale of the y-axis.

526
 527 Finally, there are opportunities to use data from CTSM simulations to augment NEON
 528 measurements. For example, measurements of soil moisture are important for calculating soil CO₂ fluxes



529 from NEON sites, but the soil moisture probes currently deployed at NEON sites do not always provide
530 reliable measurements. For example, at the Abby Road site soil moisture observations have phases of
531 erratic measurements, are missing at depth throughout much of 2020 and 2021, and have large offsets
532 when instruments were calibrated (Fig. 8, Fig. S3). By contrast, CTSM provides continuous datasets that
533 could be used to gap fill or augment ongoing NEON soil moisture measurements, although simulated
534 data may need to be bias corrected. Similarly, soil moisture controls aspects of plant phenology in CLM,
535 meaning that soil moisture measurements could help constrain or explain potential biases in simulated
536 LAI and ecosystem fluxes. At ABBY, both CTSM simulations and NEON observations show similar
537 temporal patterns – a dry-down of soil moisture during the dry summer months and followed by wetter fall
538 winter and spring months (Fig. 8; Fig. S3), although CTSM simulates wetter soils than observed at the
539 NEON site.
540



541
542 **Figure 8** Time series of volumetric soil moisture profiles that are simulated by CTSM simulations (blue) and
543 measured by NEON (orange) at different depths in soil plot 3 at the Abby Road site in Washington (ABBY) from
544 2018-2021.



545 **4. Discussion**

546 The NCAR-NEON system links models and measurements to provide a powerful suite of tools to
547 understand ecosystem properties and processes through space and time. In addition to facilitating the
548 integration of measurements and modeling, a major focus of this work is to enable new opportunities for
549 research and education by expanding access to and interaction with NCAR models and NEON data. The
550 user community can access quality-controlled and gap-filled NEON meteorological and EC flux data as
551 prototype datasets through the public-access cloud storage buckets that supports the NCAR-NEON
552 system or the Prototype Data section of the NEON Data Portal (Table 2). Additionally, the NCAR-NEON
553 system streamlines running NCAR's CTSM model and simplifies access through the containerized
554 CESM-Lab platform, bypassing the logistical challenges of porting CTSM to different computing systems.
555 It also creates customized model input data that include local site characterizations of soil and vegetation
556 using NEON data products. These capabilities allow researchers to focus their time on customizing CTSM
557 and integrating additional NEON datasets to address research questions. Combined with the visualization
558 software provided in the tutorials, the NCAR-NEON system also facilitates opportunities for teaching
559 about land-atmosphere interactions, ecology, and land modeling. Below we discuss some of the
560 synergistic enhancements this collaboration makes for NEON measurements and NCAR models as well
561 as opportunities that the NCAR-NEON system enables for research and teaching.

562 **4.1 Synergistic enhancements of NEON measurements and NCAR models**

563 The NCAR-NEON system is a collaborative partnership between observationalists and modelers
564 that enhances both NEON's measurements and NCAR's models. One typically thinks of observations as
565 improving models, but the reverse can also happen in which models inform and augment the collection of
566 measurements. For example, models require continuous meteorological input data, so gap filling the
567 missing meteorological data required to run CTSM was paramount to the success of the project. A new
568 prototype data product provided by the project is a continuous time series of meteorological data at each
569 NEON location. Comparison of modeled and measured EC fluxes identified QA/QC improvements to the
570 meteorological data needed for the model simulations, and similarly improvements to the processing of
571 the raw EC fluxes to compare with model results.

572 One issue raised in the simulations is the estimation of precipitation at grassland sites. NEON has
573 experienced issues where small amounts of noise in the raw data cause spurious trace precipitation to be
574 recorded at all primary precipitation sensors. Because secondary and throughfall precipitation buckets are
575 unaffected, there is a redundant data stream at forested sites, but these are unavailable for grassland
576 sites. An updated algorithm is expected to resolve the spurious trace precipitation issue in late 2022 with
577 back processed data available in the NEON 2024 data release. In the meantime, we manually evaluated
578 the mean annual precipitation recorded at each NEON site against other observational data networks and
579 noted locations where this issue is generating unexpectedly high or low precipitation values (Table S2).



580 Another example of how NCAR modeling improved NEON data quality comes from unusual soil
581 moisture profiles that were initially generated in preliminary simulations at the ABBY site (data not
582 shown). Upon closer inspection these patterns were found to be caused by an unusual relationship
583 between soil organic carbon content and depth at this site, which did not match related data gathered
584 during sample collection or subsequent analyses. Further investigation confirmed that the labels for the
585 soil carbon analysis subsamples had been switched for two ABBY soil horizons. The NEON soil data
586 have since been corrected and the modeled soil moisture profiles for ABBY now follow a more typical
587 pattern with surface soils drying out during the summer and less variation in soil moisture in deeper soil
588 horizons (Figs. 8, S3). There are also important differences in vertical profiles of simulated and measured
589 soil moisture, with soil moisture simulated by CTSM typically decreasing with depth while NEON soil
590 moisture observations generally increase with depth. Additional investigation is needed to determine if
591 these discrepancies extend to other sites and indicate issues with CTSM simulations or NEON data
592 products, but it does underscore a synergy in NCAR modeling and NEON measurements that deserves
593 more attention moving forward.

594 We see clear opportunities for NEON observations to help guide future model improvements,
595 especially related to potential biases in phenology (discussed above), photosynthesis (Fig. 7), and other
596 processes. Some biases in modeled processes are already documented; for example, Wozniak (2020)
597 found that CTSM underestimates maximum rates of simulated GPP compared to EC observations in
598 deciduous forest sites. This suggests that implementation of the photosynthesis scheme in CTSM has
599 parametric or structural issues that prevent high rates of GPP from occurring in the model. Auxiliary data
600 from NEON that are not always available from other EC flux towers, for example foliar chemistry, can be
601 used to update parameter values and to evaluate correlated model variables and processes. The
602 opportunities afforded by NEON's EC and auxiliary data to improve the representation of ecological
603 processes in CTSM will improve modeled carbon fluxes at NEON towers and may also ameliorate biases
604 in global simulations.

605 Finally, the NCAR-NEON system can also facilitate model-informed prioritization of future data
606 collection efforts. Models can quantify the dominant drivers of uncertainty in model parameters as well as
607 in response to environmental drivers using ensemble-based methods of parameter uncertainty
608 propagation and variance decomposition (LeBauer et al. 2013). Site-level CTSM simulations could
609 therefore help future NEON data collection campaigns to target variables that contribute the most to
610 uncertainty in modeled ecosystem fluxes and ecosystem responses to global change.

611 **4.2 Opportunities enabled for research**

612 The NCAR-NEON system enables research opportunities in the ecology, global change, and
613 Earth system science communities by: (1) Democratizing access to NCAR models that can be
614 customized to meet researchers' needs; (2) Providing a platform that leverages NEON observational
615 datasets for site-level model configuration and evaluation across the diverse range of ecosystems



616 captured in the NEON design; (3) Facilitating reproducible research workflows; and (4) Providing gap-
617 filled meteorological data and partitioned EC flux data products.

618 Through CESM-Lab, the NCAR-NEON system provides access to the full model code and
619 datasets used to run CTSM on any computing system. This means that researchers are not limited to
620 NEON locations or to the default configuration of CTSM, nor do they need access to large-scale
621 computing resources. The CTSM code can be modified and compiled within the container, so researchers
622 who wish to run simulations with new model parameterizations or with additional model features may now
623 do so from any computer. Most personal laptop computers are more than sufficient for running site level
624 simulations, even when using more computationally complex versions of the land model that include, for
625 example, ecological dynamics (using the Functionally Assembled Terrestrial Ecosystem Simulator,
626 FATES; Koven et al. 2020) or representative hillslope hydrology (Swenson et al. 2019). Advanced users
627 can run CTSM at any single point site by making their own input files. Additionally, researchers can
628 quantify the impact of adjusting model parameters and processes on terrestrial ecosystems under
629 historical and future climate scenarios. This flexibility is useful for calibrating the model to improve model
630 performance at a given site, as well as for gaining mechanistic insights into how different processes and
631 uncertainties affect ecosystem functioning. Broadening access to CTSM also allows researchers to
632 rapidly compare model output to their own observational datasets, or to existing NEON observational
633 datasets that are not yet integrated into the NCAR-NEON system.

634 Moving forward, we see additional NEON data products as providing valuable insights to the
635 NCAR-NEON system. These could include NEON measurements that are used both as model inputs
636 (foliar chemistry, phenology and LAI, and historical land use legacies) and as model validation datasets
637 (including snow depth, vertical profiles of canopy temperature, leaf water potential, litterfall rates, biomass
638 and vegetation structure, and depth profiles of soil moisture, temperature, carbon and nitrogen). Although
639 these data have not yet been integrated into the NCAR-NEON system, we are optimistic that existing
640 tools can help facilitate their integration into research opportunities. We see powerful opportunities to
641 expand on this approach to integrate information from NEON's Airborne Observation Platform (AOP) into
642 workflows that extend model capabilities beyond the relatively small footprint of the EC towers. For
643 example, the AOP light detection and ranging (LiDAR) data would provide information to initialize stand
644 structure that would be helpful for calibrating reduced complexity configurations of the CTSM-FATES
645 model (Fisher and Koven, 2020).

646 The NCAR-NEON system also promotes reproducibility of research in alignment with the FAIR
647 data principles (Wilkinson et al. 2016), addressing an ongoing challenge facing both ecology and
648 geosciences (Powers and Hampton 2019; Culina et al. 2020; Kinkade and Shepherd 2021). The NCAR-
649 NEON system makes it easy for researchers to share their research workflow as part of their publications,
650 including accompanying code and data. The containerized system also reduces the time required to
651 configure and run other researchers' workflows, thereby facilitating the process of reproducing previous
652 studies and expanding existing workflows to answer new research questions.



653 In addition to enabling opportunities for research with NCAR models, the NCAR-NEON system
654 also facilitates access to NEON data which can be used for observationally based research or research
655 using other models. For example, the gap-filled micrometeorological data and partitioned flux data
656 products provided in the NCAR-NEON system could be used in other projects related to ecological
657 forecasting and model evaluation that focuses on ecological processes and land model simulations (Best
658 et al. 2015; Collier et al. 2018; Eyring et al. 2019; Lewis et al. 2022). As latencies in publishing NEON
659 data are reduced, we intend to provide updated input and evaluation data to the NCAR-NEON system to
660 enable near-real time hindcasts of ecosystem states and fluxes. In short, we see the information that is
661 being generated through this activity as a resource to meet data-requirements of the broader Earth
662 system science community.

663 **4.3 Opportunities enabled for teaching**

664 The NCAR-NEON system makes it easy to run and visualize site-level simulations that can be
665 integrated into classroom settings. The NEON Observatory design provides a unique opportunity for
666 students to access data from world class field research sites and instrumentation in a variety of
667 ecosystems. Here we highlight two capacities in which this tool can be integrated into classroom
668 activities. The first is an interactive web-based visualization tool (Table 2). This tool does not require any
669 software or data downloads, allowing students to access and explore NEON and CTSM data without
670 running any simulations. Students can explore and compare observational and simulated data for
671 numerous fluxes at different temporal scales from 45 terrestrial NEON sites (Table S1). Classroom
672 modules can be developed to probe various ecological questions, including comparisons across sites,
673 how fluxes change seasonally, and quantification of interannual variability. Instructors can also use this
674 tool to highlight differences between models and observations, helping students to better understand how
675 we measure, simulate, and predict ecosystem processes.

676 A second opportunity for classroom activities is to run simulations using the NCAR-NEON system
677 within the CESM-Lab container. The flexible cyberinfrastructure, short simulation run times (typically less
678 than 10 minutes), and simplified coding requirements facilitate running simulations for classroom
679 applications. Technical challenges are minimal and can be reduced by using a computer lab with Docker
680 pre-installed and computers that have sufficient memory and space requirements for data downloads, or
681 by using larger-scale computing resources like university clusters or cloud computing resources. Once
682 access to the containerized computing environment is established, students can use the available
683 tutorials to run NEON tower simulations at the site of their choice and evaluate simulated fluxes against
684 observations (Table 2).

685 The NCAR-NEON system is flexible, allowing instructors to easily make additional customizations
686 for their classes. As an example, this cyberinfrastructure tool was used in a graduate level Land-Climate
687 Interactions Course at Auburn University in the 2021-2022 academic year. First, students performed
688 CTSM simulations for the Talladega National Forest site (TALL), the NEON site closest to Auburn



689 University, and compared latent heat flux simulated by CTSM with the NEON measurements using
690 system tutorials. Next, students were divided into two project groups focusing on either TALL or Ordway-
691 Swisher Biological Station (OSBS) sites to conduct parameter perturbation experiments using a tutorial
692 developed by the instructor. Students collected the relevant parameter values from the literature, updated
693 model parameter files, and performed ten CTSM simulations at each site, finding that GPP was more
694 sensitive to the selected parameters than latent heat fluxes. These classroom exercises were paired with
695 a visit to the TALL site to enrich student's experiences and motivate them to design their own
696 investigation and experiments. Exposure to the NCAR-NEON system has motivated graduate students to
697 contribute analyses, tutorials, and additional resources to the broader community. For example, one
698 graduate student compared NEON precipitation measurements with nearby NOAA sites, helping to
699 identify potentially problematic NEON sensors (Section 4.1), while another is developing a model for
700 estimating aboveground biomass using ground-based NEON data and remote sensing measurements
701 (Narine et al. 2020). These examples highlight how the NCAR-NEON system is inspiring the next
702 generation of scientists.

703 **Conclusion**

704 Deeper engagement of diverse scientific communities, removing technical barriers, and
705 increasing access to research data and tools is critical to advance Earth system science, prediction, and
706 understanding of ecosystem responses to global change. By developing cyberinfrastructure tools that
707 facilitate the easy and rapid use of measurements, models, and computing tools, the NCAR-NEON
708 system aims to enable this convergence of climate and ecological sciences and facilitates the
709 development and testing of data-driven and model-enabled scientific hypotheses. The system provides a
710 computationally simplified platform for scientific discovery and for rigorous evaluation and improvement of
711 model simulations and observational data at NEON tower sites. A particular strength of this system is the
712 auxiliary data collected by the NEON network that is used to inform site-specific model inputs and model
713 evaluation. With some effort, users can adapt this system to incorporate and simulate flux towers at other
714 research sites using the 'Processing NEON data' tools linked in Table 2 to guide data formatting. Thus,
715 future work could expand this system to include gap-filled flux data from other regional and global
716 networks like AmeriFlux and FLUXNET, allowing for broader spatial coverage. By facilitating community
717 engagement in modeling and observing terrestrial ecosystems, cyberinfrastructure tools like this are a key
718 component for building a more intellectually diverse workforce for global change research and Earth
719 system science.

720 **Code and Data availability**

721 Datasets created as part of this project are available as a NEON prototype dataset and archived at
722 NCAR's Geoscience Data Exchange (GDEX) <https://doi.org/10.5065/tmmj-sj66>. CTSM code is available



723 through the CTSM github page and archived at <https://doi.org/10.5281/zenodo.7342803>. Post processing
724 scripts that used to make figures in this manuscript are available at:
725 https://github.com/NCAR/neon_scripts.

726 **Author Contributions**

727 All authors contributed to writing and review of the software and manuscript. GBB and MSC contributed to
728 funding acquisition. DLL, WRW, NS, GBB, DD, DL, and MSC contributed to conceptualization and data
729 curation. DLL, WRW, NS, and DD contributed to formal analysis, software development, validation, and
730 visualization.

731 **Competing Interests**

732 The authors have no competing interests to declare.

733 **Acknowledgements**

734 Significant contributions to this work were made by Jim Edwards, Brian Dobbins, Erik Kluzek, and Cove
735 Sturtevant. This material is based upon work supported by the National Center for Atmospheric
736 Research, which is a major facility sponsored by the National Science Foundation (NSF) under
737 Cooperative Agreement No. 1852977 with additional support from NSF award number 2039932. The
738 National Ecological Observatory Network is a program sponsored by the NSF and operated under
739 cooperative agreement by Battelle. WRW was also supported by NSF award numbers 1926413,
740 2031238, and 2120804. SK's contributions were supported by the USDA NIFA grant 2020-67021-32476.
741 KMD's contributions were supported by NSF award numbers 1702379 and 2044818 and the USDA NIFA,
742 Hatch project 1025001.



743 **References**

- 744 Ayres, E., Colliander, A., Cosh, M. H., Roberti, J. A., Simkin, S., and Genazzio, M. A.: Validation of
745 SMAP Soil Moisture at Terrestrial National Ecological Observatory Network (NEON) Sites Show
746 Potential for Soil Moisture Retrieval in Forested Areas, *IEEE Journal of Selected Topics in*
747 *Applied Earth Observations and Remote Sensing*, 14, 10903-10918,
748 10.1109/jstars.2021.3121206, 2021.
- 749 Balch, J. K., Nagy, R. C., and Halpern, B. S.: NEON is seeding the next revolution in ecology,
750 *Frontiers in Ecology and the Environment*, 18, 3-3, 10.1002/fee.2152, 2020.
- 751 Best, M. J., Abramowitz, G., Johnson, H. R., Pitman, A. J., Balsamo, G., Boone, A., Cuntz, M.,
752 Decharme, B., Dirmeyer, P. A., Dong, J., Ek, M., Guo, Z., Haverd, V., van den Hurk, B. J. J.,
753 Nearing, G. S., Pak, B., Peters-Lidard, C., Santanello, J. A., Stevens, L., and Vuichard, N.: The
754 Plumbing of Land Surface Models Benchmarking Model Performance, *J Hydrometeorol*, 16,
755 1425-1442, 2015.
- 756 Birch, L., Schwalm, C. R., Natali, S., Lombardozzi, D., Keppel-Aleks, G., Watts, J., Lin, X., Zona, D.,
757 Oechel, W., Sachs, T., Black, T. A., and Rogers, B. M.: Addressing biases in Arctic–boreal carbon
758 cycling in the Community Land Model Version 5, *Geoscientific Model Development*, 14, 3361-
759 3382, 10.5194/gmd-14-3361-2021, 2021.
- 760 Bonan, G.: *Ecological climatology: concepts and applications*, 3, Cambridge University Press,
761 Cambridge, 2015.
- 762 Bonan, G.: *Climate change and terrestrial ecosystem modeling*, Cambridge University Press,
763 Cambridge, 2019.
- 764 Bonan, G. B.: *A Land Surface Model (LSM Version 1.0) for Ecological, Hydrological, and*
765 *Atmospheric Studies: Technical Description and User's Guide (No. NCAR/TN-417+STR)*,
766 University Corporation for Atmospheric Research, 10.5065/D6DF6P5X, 1996.
- 767 Bonan, G. B. and Doney, S. C.: Climate, ecosystems, and planetary futures: The challenge to
768 predict life in Earth system models, *Science*, 359, 10.1126/science.aam8328, 2018.
- 769 Bonan, G. B., Davis, K. J., Baldocchi, D., Fitzjarrald, D., and Neumann, H.: Comparison of the
770 NCAR LSM1 land surface model with BOREAS aspen and jack pine tower fluxes, *Journal of*
771 *Geophysical Research-Atmospheres*, 102, 29065-29075, 10.1029/96jd03095, 1997.
- 772 Bonan, G. B., Oleson, K. W., Fisher, R. A., Lasslop, G., and Reichstein, M.: Reconciling leaf
773 physiological traits and canopy flux data: Use of the TRY and FLUXNET databases in the
774 Community Land Model version 4, *Journal of Geophysical Research: Biogeosciences*, 117,
775 G02026, 10.1029/2011jg001913, 2012.
- 776 Bonan, G. B., Lawrence, P. J., Oleson, K. W., Levis, S., Jung, M., Reichstein, M., Lawrence, D. M.,
777 and Swenson, S. C.: Improving canopy processes in the Community Land Model version 4



- 778 (CLM4) using global flux fields empirically inferred from FLUXNET data, *J. Geophys. Res.*, 116,
779 G02014, 10.1029/2010jg001593, 2011.
- 780 Brock, F. V.: A Nonlinear Filter to Remove Impulse Noise from Meteorological Data, *Journal of*
781 *Atmospheric and Oceanic Technology*, 3, 51-58, 10.1175/1520-
782 0426(1986)003<0051:Anftri>2.0.Co;2, 1986.
- 783 Burns, S. P., Swenson, S. C., Wieder, W. R., Lawrence, D. M., Bonan, G. B., Knowles, J. F., and
784 Blanken, P. D.: A Comparison of the Diel Cycle of Modeled and Measured Latent Heat Flux
785 During the Warm Season in a Colorado Subalpine Forest, *Journal of Advances in Modeling Earth*
786 *Systems*, 10, 617-651, 10.1002/2017ms001248, 2018.
- 787 Collier, N., Hoffman, F. M., Lawrence, D. M., Keppel-Aleks, G., Koven, C. D., Riley, W. J., Mu, M.
788 Q., and Randerson, J. T.: The International Land Model Benchmarking (ILAMB) System: Design,
789 Theory, and Implementation, *Journal of Advances in Modeling Earth Systems*, 10, 2731-2754,
790 10.1029/2018ms001354, 2018.
- 791 Culina, A., van den Berg, I., Evans, S., and Sanchez-Tojar, A.: Low availability of code in ecology:
792 A call for urgent action, *PLoS Biol*, 18, e3000763, 10.1371/journal.pbio.3000763, 2020.
- 793 Danabasoglu, G., Lamarque, J.-F., Bacmeister, J., Bailey, D. A., DuVivier, A. K., Edwards, J.,
794 Emmons, L. K., Fasullo, J., Garcia, R., Gettelman, A., Hannay, C., Holland, M. M., Large, W. G.,
795 Lauritzen, P. H., Lawrence, D. M., Lenaerts, J. T. M., Lindsay, K., Lipscomb, W. H., Mills, M. J.,
796 Neale, R., Oleson, K. W., Otto-Bliesner, B., Phillips, A. S., Sacks, W., Tilmes, S., van Kampenhout,
797 L., Vertenstein, M., Bertini, A., Dennis, J., Deser, C., Fischer, C., Fox-Kemper, B., Kay, J. E.,
798 Kinnison, D., Kushner, P. J., Larson, V. E., Long, M. C., Mickelson, S., Moore, J. K., Nienhouse, E.,
799 Polvani, L., Rasch, P. J., and Strand, W. G.: The Community Earth System Model Version 2
800 (CESM2), *Journal of Advances in Modeling Earth Systems*, 12, e2019MS001916,
801 10.1029/2019ms001916, 2020.
- 802 Deardorff, J. W.: Efficient prediction of ground surface temperature and moisture, with
803 inclusion of a layer of vegetation, *Journal of Geophysical Research*, 83, 1889-1903,
804 10.1029/JC083iC04p01889, 1978.
- 805 Dickinson, R. E., Henderson-Sellers, A., and Kennedy, P. J.: Biosphere-atmosphere Transfer
806 Scheme (BATS) Version 1e as Coupled to the NCAR Community Climate Model (No. NCAR/TN-
807 387+STR). , University Corporation for Atmospheric Research, 10.5065/D67W6959, 1993.
- 808 Dickinson, R. E., Henderson-Sellers, A., Kennedy, P. J., & Wilson, M. F.: Biosphere-
809 atmosphere Transfer Scheme (BATS) for the NCAR Community Climate Model (No. NCAR/TN-
810 275-+STR). , 72, 10.5065/D6668B58, 1986.
- 811 Durden, D. J., Metzger, S., Chu, H., Collier, N., Davis, K. J., Desai, A. R., Kumar, J., Wieder, W. R.,
812 Xu, M., and Hoffman, F. M., Nichols, J., Verastegui, B., Maccabe, A. B., Hernandez, O., Parete-
813 Koon, S., and Ahearn, T. (Eds.): Automated Integration of Continental-Scale Observations in



- 814 Near-Real Time for Simulation and Analysis of Biosphere–Atmosphere Interactions, Springer
815 International Publishing, Cham, 204-225 pp., 10.1007/978-3-030-63393-6_14, 2020.
- 816 Eyring, V., Cox, P. M., Flato, G. M., Gleckler, P. J., Abramowitz, G., Caldwell, P., Collins, W. D.,
817 Gier, B. K., Hall, A. D., Hoffman, F. M., Hurtt, G. C., Jahn, A., Jones, C. D., Klein, S. A., Krasting, J.
818 P., Kwiatkowski, L., Lorenz, R., Maloney, E., Meehl, G. A., Pendergrass, A. G., Pincus, R., Ruane,
819 A. C., Russell, J. L., Sanderson, B. M., Santer, B. D., Sherwood, S. C., Simpson, I. R., Stouffer, R. J.,
820 and Williamson, M. S.: Taking climate model evaluation to the next level, *Nature Climate*
821 *Change*, 9, 102-110, 10.1038/s41558-018-0355-y, 2019.
- 822 Falge, E., Baldocchi, D., Olson, R., Anthoni, P., Aubinet, M., Bernhofer, C., Burba, G., Ceulemans,
823 R., Clement, R., Dolman, H., Granier, A., Gross, P., Grünwald, T., Hollinger, D., Jensen, N.-O.,
824 Katul, G., Keronen, P., Kowalski, A., Ta Lai, C., Law, B. E., Meyers, T., Moncrieff, J., Moors, E.,
825 William Munger, J., Pilegaard, K., Rannik, Ü., Rebmann, C., Suyker, A., Tenhunen, J., Tu, K.,
826 Verma, S., Vesala, T., Wilson, K., and Wofsy, S.: Gap filling strategies for long term energy flux
827 data sets, *Agricultural and Forest Meteorology*, 107, 71-77, 10.1016/s0168-1923(00)00235-5,
828 2001.
- 829 Fer, I., Gardella, A. K., Shiklomanov, A. N., Campbell, E. E., Cowdery, E. M., De Kauwe, M. G.,
830 Desai, A., Duveneck, M. J., Fisher, J. B., Haynes, K. D., Hoffman, F. M., Johnston, M. R., Kooper,
831 R., LeBauer, D. S., Mantooth, J., Parton, W. J., Poulter, B., Quaife, T., Raiho, A., Schaefer, K.,
832 Serbin, S. P., Simkins, J., Wilcox, K. R., Viskari, T., and Dietze, M. C.: Beyond ecosystem
833 modeling: A roadmap to community cyberinfrastructure for ecological data-model integration,
834 *Glob Chang Biol*, 27, 13-26, 10.1111/gcb.15409, 2021.
- 835 Finkenbiner, C. E., Li, B., Spencer, L., Butler, Z., Haagsma, M., Fiorella, R. P., Allen, S. T.,
836 Anderegg, W., Still, C. J., Noone, D., Bowen, G. J., and Good, S. P.: The NEON Daily Isotopic
837 Composition of Environmental Exchanges Dataset, *Scientific Data*, 9, 353, 10.1038/s41597-022-
838 01412-4, 2022.
- 839 Fisher, R. A. and Koven, C. D.: Perspectives on the Future of Land Surface Models and the
840 Challenges of Representing Complex Terrestrial Systems, *Journal of Advances in Modeling Earth*
841 *Systems*, 12, e2018MS001453, 10.1029/2018ms001453, 2020.
- 842 Hinckley, E.-L. S., Anderson, S. P., Baron, J. S., Blanken, P. D., Bonan, G. B., Bowman, W. D.,
843 Elmendorf, S. C., Fierer, N., Fox, A. M., Goodman, K. J., Jones, K. D., Lombardozzi, D. L., Lunch, C.
844 K., Neff, J. C., SanClements, M. D., Suding, K. N., and Wieder, W. R.: Optimizing Available
845 Network Resources to Address Questions in Environmental Biogeochemistry, *BioScience*, 66,
846 317-326, 10.1093/biosci/biw005, 2016.
- 847 Hurrell, J. W., Holland, M. M., Gent, P. R., Ghan, S., Kay, J. E., Kushner, P. J., Lamarque, J. F.,
848 Large, W. G., Lawrence, D., Lindsay, K., Lipscomb, W. H., Long, M. C., Mahowald, N., Marsh, D.
849 R., Neale, R. B., Rasch, P., Vavrus, S., Vertenstein, M., Bader, D., Collins, W. D., Hack, J. J., Kiehl,
850 J., and Marshall, S.: The Community Earth System Model: A Framework for Collaborative



- 851 Research, *Bulletin of the American Meteorological Society*, 94, 1339-1360, 10.1175/bams-d-12-
852 00121.1, 2013.
- 853 Jung, M., Schwalm, C., Migliavacca, M., Walther, S., Camps-Valls, G., Koirala, S., Anthoni, P.,
854 Besnard, S., Bodesheim, P., Carvalhais, N., Chevallier, F., Gans, F., Goll, D. S., Haverd, V., Köhler,
855 P., Ichii, K., Jain, A. K., Liu, J., Lombardozzi, D., Nabel, J. E. M. S., Nelson, J. A., O'Sullivan, M.,
856 Pallandt, M., Papale, D., Peters, W., Pongratz, J., Rödenbeck, C., Sitch, S., Tramontana, G.,
857 Walker, A., Weber, U., and Reichstein, M.: Scaling carbon fluxes from eddy covariance sites to
858 globe: synthesis and evaluation of the FLUXCOM approach, *Biogeosciences*, 17, 1343-1365,
859 10.5194/bg-17-1343-2020, 2020.
- 860 Kinkade, D. and Shepherd, A.: Geoscience data publication: Practices and perspectives on
861 enabling the FAIR guiding principles, *Geoscience Data Journal*, 9, 177-186, 10.1002/gdj3.120,
862 2021.
- 863 Koven, C. D., Knox, R. G., Fisher, R. A., Chambers, J. Q., Christoffersen, B. O., Davies, S. J., Detto,
864 M., Dietze, M. C., Faybishenko, B., Holm, J., Huang, M., Kovenock, M., Kueppers, L. M., Lemieux,
865 G., Massoud, E., McDowell, N. G., Muller-Landau, H. C., Needham, J. F., Norby, R. J., Powell, T.,
866 Rogers, A., Serbin, S. P., Shuman, J. K., Swann, A. L. S., Varadharajan, C., Walker, A. P., Wright, S.
867 J., and Xu, C.: Benchmarking and parameter sensitivity of physiological and vegetation dynamics
868 using the Functionally Assembled Terrestrial Ecosystem Simulator (FATES) at Barro Colorado
869 Island, Panama, *Biogeosciences*, 17, 3017-3044, 10.5194/bg-17-3017-2020, 2020.
- 870 Kyker-Snowman, E., Lombardozzi, D. L., Bonan, G. B., Cheng, S. J., Dukes, J. S., Frey, S. D.,
871 Jacobs, E. M., McNellis, R., Rady, J. M., Smith, N. G., Thomas, R. Q., Wieder, W. R., and Grandy,
872 A. S.: Increasing the spatial and temporal impact of ecological research: A roadmap for
873 integrating a novel terrestrial process into an Earth system model, *Glob Chang Biol*, 28, 665-
874 684, 10.1111/gcb.15894, 2021.
- 875 Lawrence, D. M., Fisher, R. A., Koven, C. D., Oleson, K. W., Swenson, S. C., Bonan, G., Collier, N.,
876 Ghimire, B., Kampenhout, L., Kennedy, D., Kluzek, E., Lawrence, P. J., Li, F., Li, H., Lombardozzi,
877 D., Riley, W. J., Sacks, W. J., Shi, M., Vertenstein, M., Wieder, W. R., Xu, C., Ali, A. A., Badger, A.
878 M., Bisht, G., Broeke, M., Brunke, M. A., Burns, S. P., Buzan, J., Clark, M., Craig, A., Dahlin, K.,
879 Drewniak, B., Fisher, J. B., Flanner, M., Fox, A. M., Gentine, P., Hoffman, F., Keppel-Aleks, G.,
880 Knox, R., Kumar, S., Lenaerts, J., Leung, L. R., Lipscomb, W. H., Lu, Y., Pandey, A., Pelletier, J. D.,
881 Perket, J., Randerson, J. T., Ricciuto, D. M., Sanderson, B. M., Slater, A., Subin, Z. M., Tang, J.,
882 Thomas, R. Q., Val Martin, M., and Zeng, X.: The Community Land Model Version 5: Description
883 of New Features, Benchmarking, and Impact of Forcing Uncertainty, *Journal of Advances in*
884 *Modeling Earth Systems*, 11, 4245-4287, 10.1029/2018ms001583, 2019.
- 885 LeBauer, D. S., Wang, D., Richter, K. T., Davidson, C. C., and Dietze, M. C.: Facilitating feedbacks
886 between field measurements and ecosystem models, *Ecological Monographs*, 83, 133-154,
887 10.1890/12-0137.1, 2013.



- 888 Levis, S., Bonan, G. B., Vertenstein, M., and Oleson, K. W.: The Community Land Model's
889 Dynamic Global Vegetation Model (CLM-DGVM): Technical description and user's guide. NCAR
890 Technical Note NCAR/TN-459+IA., National Center for Atmospheric Research, Boulder, CO. ,
891 10.5065/D6P26W36, 2004.
- 892 Lewis, A. S. L., Rollinson, C. R., Allyn, A. J., Ashander, J., Brodie, S., Brookson, C. B., Collins, E.,
893 Dietze, M. C., Gallinat, A. S., Juvigny-Khenafou, N., Koren, G., McGlenn, D. J., Moustahfid, H.,
894 Peters, J. A., Record, N. R., Robbins, C. J., Tonkin, J., and Wardle, G. M.: The power of forecasts
895 to advance ecological theory, *Methods in Ecology and Evolution*, n/a, 10.1111/2041-
896 210x.13955, 2022.
- 897 Li, X., Melaas, E., Carrillo, C. M., Ault, T., Richardson, A. D., Lawrence, P., Friedl, M. A.,
898 Seyednasrollah, B., Lawrence, D. M., and Young, A. M.: A Comparison of Land Surface
899 Phenology in the Northern Hemisphere Derived from Satellite Remote Sensing and the
900 Community Land Model, *J Hydrometeorol*, 23, 859-873, 10.1175/jhm-d-21-0169.1, 2022.
- 901 Lombardozzi, D. L., Bonan, G. B., Smith, N. G., Dukes, J. S., and Fisher, R. A.: Temperature
902 acclimation of photosynthesis and respiration: A key uncertainty in the carbon cycle-climate
903 feedback, *Geophysical Research Letters*, 42, 8624-8631, 10.1002/2015GL065934., 2015.
- 904 Metzger, S., Ayres, E., Durden, D., Florian, C., Lee, R., Lunch, C., Luo, H., Pingintha-Durden, N.,
905 Roberti, J. A., SanClements, M., Sturtevant, C., Xu, K., and Zulueta, R. C.: From NEON Field Sites
906 to Data Portal: A Community Resource for Surface–Atmosphere Research Comes Online,
907 *Bulletin of the American Meteorological Society*, 100, 2305-2325, 10.1175/bams-d-17-0307.1,
908 2019.
- 909 Miles, A., jakirkham, Bussonnier, M., Moore, J., Orfanos, D. P., Fulton, A., Bourbeau, J., Lee, G.,
910 Patel, Z., Bennett, D., Rocklin, M., Abernathey, R., Andrade, E. S. d., Durant, M., Schut, V.,
911 Dussin, R., Kristensen, M. R. B., Chaudhary, S., Barnes, C., Nunez-Iglesias, J., Williams, B., Mohar,
912 B., Noyes, C., Bell, R., hailiangzhang, shikharsg, Jelenak, A., Sansal, A., and Banihirwe, A.: zarr-
913 developers/zarr-python: v2.13.0 Zenodo, 10.5281/zenodo.7104413, 2022.
- 914 Moffat, A. M., Papale, D., Reichstein, M., Hollinger, D. Y., Richardson, A. D., Barr, A. G.,
915 Beckstein, C., Braswell, B. H., Churkina, G., Desai, A. R., Falge, E., Gove, J. H., Heimann, M., Hui,
916 D., Jarvis, A. J., Kattge, J., Noormets, A., and Stauch, V. J.: Comprehensive comparison of gap-
917 filling techniques for eddy covariance net carbon fluxes, *Agricultural and Forest Meteorology*,
918 147, 209-232, 10.1016/j.agrformet.2007.08.011, 2007.
- 919 Moon, M., Richardson, A. D., Milliman, T., and Friedl, M. A.: A high spatial resolution land
920 surface phenology dataset for AmeriFlux and NEON sites, *Scientific Data*, 9, 448,
921 10.1038/s41597-022-01570-5, 2022.
- 922 Narine, L. L., Popescu, S. C., and Malambo, L.: Using ICESat-2 to Estimate and Map Forest
923 Aboveground Biomass: A First Example, 10.3390/rs12111824, 2020.



- 924 National Academies of Sciences, E. and Medicine: Next Generation Earth Systems Science at the
925 National Science Foundation, The National Academies Press, Washington, DC, 136 pp.,
926 10.17226/26042, 2022.
- 927 NEON (National Ecological Observatory Network). NCAR-NEON gap-filled data, v2
928 (10.48443/8w20-r938). <https://doi.org/10.48443/8w20-r938>. Dataset accessed from
929 <https://data.neonscience.org> on February 13, 2023
- 930 Oleson, K., Lawrence, D., Bonan, G., Drewniak, B., Huang, M., Koven, C., Levis, S., Li, F., Riley,
931 W., and Subin, Z.: Technical description of version 4.0 of the Community Land Model (CLM),
932 NCAR Tech, Notes (NCAR/TN-478+ STR), 605, 2010.
- 933 Oleson, K., Dai, Y., Bonan, G. B., Bosilovich, M., Dickinson, R. E., Dirmeyer, P., Hoffman, F.,
934 Houser, P., Levis, S., Niu, G.-Y., Thornton, P., Vertenstein, M., Z.-L., Y., and Zeng, X.: Technical
935 Description of the Community Land Model (CLM) (No. NCAR/TN-461+STR), University
936 Corporation for Atmospheric Research, 185, 10.5065/D6N877R0, 2004.
- 937 Oleson, K., Lawrence, D. M., Bonan, G. B., Drewniak, B., Huang, M., Koven, C. D., Levis, S., Li, F.,
938 Riley, W. J., Subin, Z. M., Swenson, S., Thornton, P. E., Bozbiyik, A., Fisher, R., Heald, C. L.,
939 Kluzek, E., Lamarque, J. F., Lawrence, P. J., Leung, L. R., Lipscomb, W., Muszala, S. P., Ricciuto, D.
940 M., Sacks, W. J., Sun, Y., Tang, J., and Yang, Z. L.: Technical description of version 4.5 of the
941 Community Land Model (CLM). NCAR Technical Note NCAR/TN-503+STR, 10.5065/D6RR1W7M,
942 2013.
- 943 Pastorello, G., Trotta, C., Canfora, E., Chu, H., Christianson, D., Cheah, Y.-W., Poindexter, C.,
944 Chen, J., Elbashandy, A., Humphrey, M., Isaac, P., Polidori, D., Reichstein, M., Ribeca, A., van
945 Ingen, C., Vuichard, N., Zhang, L., Amiro, B., Ammann, C., Arain, M. A., Ardö, J., Arkebauer, T.,
946 Arndt, S. K., Arriga, N., Aubinet, M., Aurela, M., Baldocchi, D., Barr, A., Beamesderfer, E.,
947 Marchesini, L. B., Bergeron, O., Beringer, J., Bernhofer, C., Berveiller, D., Billesbach, D., Black, T.
948 A., Blanken, P. D., Bohrer, G., Boike, J., Bolstad, P. V., Bonal, D., Bonnefond, J.-M., Bowling, D. R.,
949 Bracho, R., Brodeur, J., Brümmer, C., Buchmann, N., Burban, B., Burns, S. P., Buysse, P., Cale, P.,
950 Cavagna, M., Cellier, P., Chen, S., Chini, I., Christensen, T. R., Cleverly, J., Collalti, A., Consalvo,
951 C., Cook, B. D., Cook, D., Coursolle, C., Cremonese, E., Curtis, P. S., D'Andrea, E., da Rocha, H.,
952 Dai, X., Davis, K. J., Cinti, B. D., Grandcourt, A. d., Ligne, A. D., De Oliveira, R. C., Delpierre, N.,
953 Desai, A. R., Di Bella, C. M., Tommasi, P. d., Dolman, H., Domingo, F., Dong, G., Dore, S., Duce,
954 P., Dufrêne, E., Dunn, A., Dušek, J., Eamus, D., Eichelmann, U., ElKhidir, H. A. M., Eugster, W.,
955 Ewenz, C. M., Ewers, B., Famulari, D., Fares, S., Feigenwinter, I., Feitz, A., Fensholt, R., Filippa,
956 G., Fischer, M., Frank, J., Galvagno, M., Gharun, M., Gianelle, D., Gielen, B., Gioli, B., Gitelson,
957 A., Goded, I., Goeckede, M., Goldstein, A. H., Gough, C. M., Goulden, M. L., Graf, A., Griebel, A.,
958 Gruening, C., Grünwald, T., Hammerle, A., Han, S., Han, X., Hansen, B. U., Hanson, C., Hatakka,
959 J., He, Y., Hehn, M., Heinesch, B., Hinko-Najera, N., Hörtnagl, L., Hutley, L., Ibrom, A., Ikawa, H.,
960 Jackowicz-Korczynski, M., Janouš, D., Jans, W., Jassal, R., Jiang, S., Kato, T., Khomik, M., Klatt, J.,
961 Knohl, A., Knox, S., Kobayashi, H., Koerber, G., Kolle, O., Kosugi, Y., Kotani, A., Kowalski, A.,
962 Kruijt, B., Kurbatova, J., Kutsch, W. L., Kwon, H., Launiainen, S., Laurila, T., Law, B., Leuning, R.,
963 Li, Y., Liddell, M., Limousin, J.-M., Lion, M., Liska, A. J., Lohila, A., López-Ballesteros, A., López-



- 964 Blanco, E., Loubet, B., Loustau, D., Lucas-Moffat, A., Lüers, J., Ma, S., Macfarlane, C., Magliulo,
965 V., Maier, R., Mammarella, I., Manca, G., Marcolla, B., Margolis, H. A., Marras, S., Massman, W.,
966 Mastepanov, M., Matamala, R., Matthes, J. H., Mazzenga, F., McCaughey, H., McHugh, I.,
967 McMillan, A. M. S., Merbold, L., Meyer, W., Meyers, T., Miller, S. D., Minerbi, S., Moderow, U.,
968 Monson, R. K., Montagnani, L., Moore, C. E., Moors, E., Moreaux, V., Moureaux, C., Munger, J.
969 W., Nakai, T., Neiryck, J., Nestic, Z., Nicolini, G., Noormets, A., Northwood, M., Nosetto, M.,
970 Nouvellon, Y., Novick, K., Oechel, W., Olesen, J. E., Ourcival, J.-M., Papuga, S. A., Parmentier, F.-
971 J., Paul-Limoges, E., Pavelka, M., Peichl, M., Pendall, E., Phillips, R. P., Pilegaard, K., Pirk, N.,
972 Posse, G., Powell, T., Prasse, H., Prober, S. M., Rambal, S., Rannik, Ü., Raz-Yaseef, N., Rebmann,
973 C., Reed, D., Dios, V. R. d., Restrepo-Coupe, N., Reverter, B. R., Roland, M., Sabbatini, S., Sachs,
974 T., Saleska, S. R., Sánchez-Cañete, E. P., Sanchez-Mejia, Z. M., Schmid, H. P., Schmidt, M.,
975 Schneider, K., Schrader, F., Schroder, I., Scott, R. L., Sedláč, P., Serrano-Ortíz, P., Shao, C., Shi, P.,
976 Shironya, I., Siebicke, L., Šigut, L., Silberstein, R., Sirca, C., Spano, D., Steinbrecher, R., Stevens,
977 R. M., Sturtevant, C., Suyker, A., Tagesson, T., Takanashi, S., Tang, Y., Tapper, N., Thom, J.,
978 Tomassucci, M., Tuovinen, J.-P., Urbanski, S., Valentini, R., van der Molen, M., van Gorsel, E.,
979 van Huissteden, K., Varlagin, A., Verfaillie, J., Vesala, T., Vincke, C., Vitale, D., Vygodskaya, N.,
980 Walker, J. P., Walter-Shea, E., Wang, H., Weber, R., Westermann, S., Wille, C., Wofsy, S.,
981 Wohlfahrt, G., Wolf, S., Woodgate, W., Li, Y., Zampedri, R., Zhang, J., Zhou, G., Zona, D.,
982 Agarwal, D., Biraud, S., Torn, M., and Papale, D.: The FLUXNET2015 dataset and the ONEFlux
983 processing pipeline for eddy covariance data, *Scientific Data*, 7, 225, 10.1038/s41597-020-0534-
984 3, 2020.
- 985 Powers, S. M. and Hampton, S. E.: Open science, reproducibility, and transparency in ecology,
986 *Ecol Appl*, 29, e01822, 10.1002/eap.1822, 2019.
- 987 Reichstein, M., Falge, E., Baldocchi, D., Papale, D., Aubinet, M., Berbigier, P., Bernhofer, C.,
988 Buchmann, N., Gilmanov, T., Granier, A., Grunwald, T., Havrankova, K., Ilvesniemi, H., Janous,
989 D., Knohl, A., Laurila, T., Lohila, A., Loustau, D., Matteucci, G., Meyers, T., Miglietta, F., Ourcival,
990 J.-M., Pumpanen, J., Rambal, S., Rotenberg, E., Sanz, M., Tenhunen, J., Seufert, G., Vaccari, F.,
991 Vesala, T., Yakir, D., and Valentini, R.: On the separation of net ecosystem exchange into
992 assimilation and ecosystem respiration: review and improved algorithm, *Global Change Biology*,
993 11, 1424-1439, 10.1111/j.1365-2486.2005.001002.x, 2005.
- 994 Richardson, A.D., Hufkens, K., Milliman, T., Aubrecht, D.M., Chen, M., Gray, J.M., Johnston,
995 M.R., Keenan, T.F., Klosterman, S.T., Kosmala, M., Melaas, E.K., Friedl, M.A., and Frohling, S.:
996 Tracking vegetation phenology across diverse North American biomes using PhenoCam
997 imagery, *Scientific Data* 5, Article number: 180028. doi:10.1038/sdata.2018.28, 2018.
998
- 999 Richardson, L. F.: *Weather prediction by numerical process*, Cambridge University Press,
1000 Cambridge 1922.
- 1001 Shepherd, A., Jones, M. B., Richard, S., Jarboe, N., Vieglais, D., Fils, D., Duerr, R., Verhey, C.,
1002 Minch, M., Mecum, B., and Bentley, N.: *Science-on-Schema.org v1.3.0*, Zenodo,
1003 10.5281/zenodo.6502539, 2022.



- 1004 Starkenburg, D., Metzger, S., Fochesatto, G. J., Alfieri, J. G., Gens, R., Prakash, A., and Cristóbal,
1005 J.: Assessment of Despiking Methods for Turbulence Data in Micrometeorology, *Journal of*
1006 *Atmospheric and Oceanic Technology*, 33, 2001-2013, 10.1175/jtech-d-15-0154.1, 2016.
- 1007 Stöckli, R., Lawrence, D. M., Niu, G. Y., Oleson, K. W., Thornton, P. E., Yang, Z. L., Bonan, G. B.,
1008 Denning, A. S., and Running, S. W.: Use of FLUXNET in the Community Land Model
1009 development, *Journal of Geophysical Research: Biogeosciences*, 113, 10.1029/2007jg000562,
1010 2008.
- 1011 Swann, A. L. S., Laguë, M. M., Garcia, E. S., Field, J. P., Breshears, D. D., Moore, D. J. P., Saleska,
1012 S. R., Stark, S. C., Villegas, J. C., Law, D. J., and Minor, D. M.: Continental-scale consequences of
1013 tree die-offs in North America: identifying where forest loss matters most, *Environ Res Lett*, 13,
1014 055014, 10.1088/1748-9326/aaba0f, 2018.
- 1015 Swenson, S. C., Clark, M., Fan, Y., Lawrence, D. M., and Perket, J.: Representing Intra-Hillslope
1016 Lateral Subsurface Flow in the Community Land Model, *Journal of Advances in Modeling Earth*
1017 *Systems*, 11, 10.1029/2019ms001833, 2019.
- 1018 van der Horst, S. V. J., Pitman, A. J., De Kauwe, M. G., Ukkola, A., Abramowitz, G., and Isaac, P.:
1019 How representative are FLUXNET measurements of surface fluxes during temperature
1020 extremes?, *Biogeosciences*, 16, 1829-1844, 10.5194/bg-16-1829-2019, 2019.
- 1021 Wieder, W. R., Knowles, J. F., Blanken, P. D., Swenson, S. C., and Suding, K. N.: Ecosystem
1022 function in complex mountain terrain: Combining models and long-term observations to
1023 advance process-based understanding, *Journal of Geophysical Research: Biogeosciences*, 122,
1024 825-845, 10.1002/2016jg003704, 2017.
- 1025 Wilkinson, M. D., Dumontier, M., Aalbersberg, I. J., Appleton, G., Axton, M., Baak, A., Blomberg,
1026 N., Boiten, J.-W., da Silva Santos, L. B., Bourne, P. E., Bouwman, J., Brookes, A. J., Clark, T.,
1027 Crosas, M., Dillo, I., Dumon, O., Edmunds, S., Evelo, C. T., Finkers, R., Gonzalez-Beltran, A., Gray,
1028 A. J. G., Groth, P., Goble, C., Grethe, J. S., Heringa, J., 't Hoen, P. A. C., Hoof, R., Kuhn, T., Kok,
1029 R., Kok, J., Lusher, S. J., Martone, M. E., Mons, A., Packer, A. L., Persson, B., Rocca-Serra, P.,
1030 Roos, M., van Schaik, R., Sansone, S.-A., Schultes, E., Sengstag, T., Slater, T., Strawn, G., Swertz,
1031 M. A., Thompson, M., van der Lei, J., van Mulligen, E., Velterop, J., Waagmeester, A.,
1032 Wittenburg, P., Wolstencroft, K., Zhao, J., and Mons, B.: The FAIR Guiding Principles for
1033 scientific data management and stewardship, *Scientific Data*, 3, 160018,
1034 10.1038/sdata.2016.18, 2016.
- 1035 Wozniak, M. C., Bonan, G. B., Keppel-Aleks, G., and Steiner, A. L.: Influence of Vertical
1036 Heterogeneities in the Canopy Microenvironment on Interannual Variability of Carbon Uptake
1037 in Temperate Deciduous Forests, *Journal of Geophysical Research: Biogeosciences*, 125,
1038 e2020JG005658, 10.1029/2020jg005658, 2020.

<https://doi.org/10.5194/egusphere-2023-271>

Preprint. Discussion started: 25 April 2023

© Author(s) 2023. CC BY 4.0 License.



1039 Wutzler, T., Lucas-Moffat, A., Migliavacca, M., Knauer, J., Sickel, K., Šigut, L., Menzer, O., and
1040 Reichstein, M.: Basic and extensible post-processing of eddy covariance flux data with
1041 REddyProc, *Biogeosciences*, 15, 5015-5030, 10.5194/bg-15-5015-2018, 2018.

1042